Journal of Structural Chemistry. Vol. 57, No. 2, pp. 213-237, 2016.

Devoted to the 80th anniversary of Professor S. P. Gabuda

GABUDA'S MODEL OF AVERAGING LOCAL MAGNETIC FIELDS IN SOLID-STATE NMR. THE MOBILITY OF ATOMS AND MOLECULES

S. G. Kozlova[1], N. A. Sergeev[2], and V. M. Buznik[3,4]

UDC 544.2

The review presents the main results of the studies of Prof. S. P. Gabuda, which were devoted to the NMR investigation of the mobility of atoms and molecules. The basic principles of his model for averaging local magnetic fields under the conditions of atomic and molecular mobility are outlined. This model provides a relationship between the parameters of these fields with the structural features of the mobility of atoms and molecules and intermolecular interactions. Ionic and molecular crystals, zeolites, molecular sieves, hydrated proteins, and so on are considered. Phase transitions in guest subsystems, effects of dynamic disordering and correlated electron motion on the mobility of atoms and molecules and their location are discussed.

DOI: 10.1134/S0022476616020013

Keywords: NMR, mobility of atoms and molecules, solids, minerals, sorbents, hydrated proteins.

INTRODUCTION

The basic principle of the NMR method of nuclei with the spin $I = 1/2$ is the measurement of local magnetic fields on nuclei whose source as the magnetic moments of other nuclei and electrons, electron orbital currents, etc. [1, 2]. The internal mobility of atoms results in the averaging, and consequently, a decrease in local magnetic fields on resonating nuclei if the correlation frequency of nuclear motion ν_c is larger than the NMR line width ($\nu_c \geq 10^4$ Hz) [3]. In diamagnetic crystals where the electronic moments are coupled and their effect is excluded, the main source of local magnetic fields (h^{loc}) is the magnetic moments of the neighboring atomic nuclei (μ) of a solid under study. For instance, for crystal hydrates the NMR spectra on the nuclei of hydrogen atoms of water molecules the resonance line has a shape of the Pake doublet with the splitting $2h^{loc}$ due to the intramolecular dipole interaction of the magnetic moments of two proton nuclei [4]. The characteristic shape of the ^{1}H NMR spectra for "fixed" water molecules in a polycrystal (e.g., in a gypsum polycrystal) is depicted in Fig. 1 (left). The maximum splitting $2h^{loc}$ (z component) in the doublets of these spectra reaches 21-22 G [4]. The center of the figure depicts the NMR spectrum of water at the intense mobility in the crystal lattice ($2h^{loc}$ is less than 10 G)

[1]Nikolaev Institute of Inorganic Chemistry, Siberian Branch, Russian Academy of Sciences, Novosibirsk, Russia; sgk@niic.nsc.ru. [2]Institute of Physics, University of Szczecin, Poland. [3]All-Russian Scientific Research Institute of Aviation Materials, Moscow, Russia. [4]Tomsk National Research State University, Russia. Translated from *Zhurnal Strukturnoi Khimii*, Vol. 57, No. 2, pp. 230-254, March-April, 2016. Original article submitted September 15, 2015.

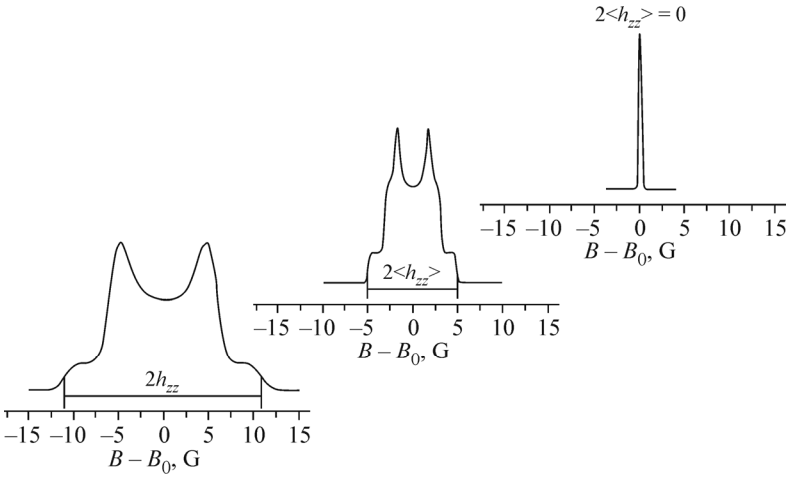

Fig. 1. Comparison of the typical ^{1}H NMR spectrum in polycrystals for water molecules at their intensive mobility in the crystal lattice (in the center) with similar spectra of homogeneous states (solid and liquid). $2h_{zz}$ is the z component of $2h^{loc}$.

[5-8]. At the right there is a typical spectrum of the fluid, which represents a single narrow line ($\langle h^{loc}\rangle = 0$). Note also the the same line can be observed in the crystal lattice, too. The reason for this is that when there is the internal mobility, the time-averaged local magnetic field $\langle h^{loc}\rangle$ is experimentally fixed on the resonating nucleus in the crystal rather than the instant local magnetic field h^{loc}. It is determined by a certain motion mechanism, therefore from the analysis of $\langle h^{loc}\rangle$ values and their angular dependence with respect to the external magnetic field it is possible to find the motion path of water molecules in various hydrated objects.

Attempts to interpret narrow doublets measured in crystal hydrates at high temperatures have repeatedly been made [5-9]. In [5] the narrowing of the spectrum in hydrates was related to the appearance of two degrees of freedom in water molecules: rotation about the twofold symmetry axis of the molecule and simultaneous precession of this axis about some distinguished direction in the crystal. The precession angle determines the average doublet splitting $2\langle h^{loc}\rangle$. In [6, 9] a model was proposed for the free anisotropic rotation of water molecules, which was characterized by a continuous probability distribution function of different orientations of vectors linking the magnetic moments of hydrogen nuclei in a water molecule (**p–p** vectors) relative to the crystal axes. The form of this function determines both magnitude and angular dependence of $2\langle h^{loc}\rangle$. In [7] the probability distribution function of different orientations of the **p–p** vector was assumed to be not zero only for some crystal lattice directions fixed relative to the crystal, as for the reorientational motion. The mentioned models satisfactorily explain only few of experimental facts associated with the appearance of narrow doublets. Here it is necessary to introduce various assumptions such as, e.g., the ensemble of water molecules in the crystal is very weakly bound to the crystal lattice and behaves as an almost free system of rotating molecules. In order to explain the single doublets in systems with several structurally inequivalent water molecules at $\nu_c \geq 10^4$ Hz it is needed to suppose that the motion character is identical for all water molecules and is completely independent on their nearest environment.

In [10] S. P. Gabuda and A. G. Lundin were one of the first who paid attention to that the angular dependences of all narrowed doublets observed in crystal hydrates could be assigned to one of the three dependences

$$2\langle h^{loc}\rangle = A(3\cos^2\gamma - 1) + B\sin^2\gamma\cos^2\varphi, \quad (1)$$

$$2\langle h^{loc}\rangle = C(3\cos^2\gamma - 1), \quad (2)$$

$$2\langle h^{loc}\rangle = 0. \quad (3)$$

In (1) and (2) the γ and φ angles are the spherical angles governing the orientation of the magnetic field vector; A, B, C are the structural parameters independent of γ and φ.

S. P. Gabuda showed for the first time [11] that the occurrence of only three possible angular dependences of narrowed doublets is related to the symmetry of the arrangement of **p–p** vectors of a water molecule moving in the crystal.

He also proposed a simple and physically vivid model for the calculation of narrowed doublet splittings, which was based on the vacancy mechanism of diffusion of water molecules [10, 11]. The model of averaging the local magnetic fields (Gabuda's model) made it possible to relate the main characteristics of NMR spectra of a crystal with the presence of mobility with those of NMR spectra of a crystal in the absence of internal mobility [10, 11]. The absence of mobility has an alleged meaning here and corresponds to the state in which the crystal temperature is so lowered that the mean motion frequency of molecules $\nu_c << 10^4$ Hz and their motion already does not affect the NMR spectrum (i.e., h^{loc} is not averaged).

NMR SPECTRA AND S. P. GABUDA'S MODEL OF AVERAGING LOCAL MAGNETIC FIELDS

Basic principles of the model

As mentioned above, for the majority of crystals in which the water diffusion mechanism has the vacancy character, at a frequency of diffusion jumps of molecules of about 10^4-10^6 Hz the dynamic narrowing of the NMR spectra occurs [12]. In each of the equilibrium positions occupied during the diffusion process the water molecule is oriented in a certain way for this site (e.g., for the local energy minimum to appear in the molecular position due to the formation of hydrogen bonds, the interaction between the ions and polar groups of molecules, or fluctuations of their electron density, and other mechanisms). If the time of the transition from one site to another is much less than the lifetime of the molecule in each site, then the averaging over time h^{loc} is reduced to the mean value $\langle h^{loc} \rangle$ for the ensemble of molecules in accordance to their positions and orientations of **p–p** vectors. If in the diffusion process the **p–p** vector takes m positions permitted by the structure, each of which is characterized by the relative weight p_i (p_i is the statistical probability of the occupation of the i-th site, satisfying the condition $\sum_{i=1}^{m} p_i = 1$) and the local magnetic field h_i^{loc}, then the average value of the intramolecular part of the local field is described by the expression [10]

$$\langle h^{loc} \rangle = \sum_{i=1}^{m} p_i h_i^{loc}, \tag{4}$$

where

$$h_i^{loc} = \pm \frac{3\gamma\hbar}{4} \frac{3\cos^2 \theta_i - 1}{R_i^3}. \tag{5}$$

Here R_i is the distance between two magnetic moments of protons of water molecules; γ is gyromagnetic ratio; $\hbar$ is Planck's constant; θ_i is the angle between the directions of the external magnetic field and the **p–p** vector in the i-th position. Expression (4) in the general form is a relationship of the averaged local field $\langle h^{loc} \rangle$ with the structural parameters R_i, p_i, and θ_i which determine the location of water molecules in the crystal and the diffusion mechanism. It is worth noting that $\langle h^{loc} \rangle$ is directly related to R_i, p_i, and θ_i that can be found from the NMR spectra at low temperatures. At low temperatures, when diffusion proceeds slowly, each of the possible structurally inequivalent positions of a water molecule (m) gives its doublet (i). Relative intensities p_i and angular dependences of these doublets are found from the experimental NMR spectra.

The intermolecular part $\langle h^{loc} \rangle$ is found similarly to (4), but the distances between magnetic moments are much larger than R_i values and mainly affect only the widths of spectral line components [13, 14].

Averaged local magnetic fields and crystal symmetries

Expression (4) is the relationship between the averaged local magnetic field with the structural parameters R_i, p_i, and θ_i. It must be emphasized that expression (5) entering into (4) was obtained in the assumption that the z axis of the rectangular system of coordinates is chosen in the crystal along the direction of the external magnetic field H_0 [4]. When the crystal orientation is changed in the external magnetic field, θ_i angles vary between the direction of the external magnetic field and **p–p** vectors in the i-th positions of a water molecule, which creates certain difficulties in the calculation of $\langle h^{loc} \rangle$ by formulas

(4) and (5). Moreover, as shown in [11, 15], the character of the angular dependence of the narrowed doublet is determined by the symmetry of the mutual arrangement of **p**–**p** vectors of a diffusing water molecule, which is unambiguously related to the crystal symmetry. In order to reveal this dependence it is convenient to use the magnetic dipole-dipole interaction tensor (D_{kl}) [15]

$$D_{kl}^{i} = (3r_k^i r_l^i - \delta_{kl}) / \mathbf{R}_i^3 = \frac{1}{\mathbf{R}_i^3}\begin{pmatrix} 3x_i^2 - 1 & 3x_i y_i & 3x_i z_i \\ 3x_i y_i & 3y_i^2 - 1 & 3y_i z_i \\ 3x_i z_i & 3y_i z_i & 3z_i^2 - 1 \end{pmatrix}, \tag{6}$$

where $k, l = x, y, z$; δ_{kl} is the Kronecker delta, and $r_x^i \equiv x_i$, $r_y^i \equiv y_i$, $r_z^i \equiv z_i$ are the directional cosines of the internuclear vector $\mathbf{R}_i$.

It is easy to see that the D_{kl}^i tensor is axially symmetric with the zero trace

$$D_{xx}^i + D_{yy}^i + D_{zz}^i = 0. \tag{7}$$

Since in the system of coordinates in which the external magnetic field is directed along the z axis we have $\cos\theta_i \equiv r_z^i$, from formulas (5) and (4) we find

$$h_i^{\text{loc}} = \pm\frac{3\gamma\hbar}{4} D_{zz}^i, \tag{8}$$

$$2\langle h^{\text{loc}}\rangle = W\langle D_{zz}\rangle, \tag{9}$$

where $W = 3\gamma\hbar/2$ and

$$\langle D_{zz}\rangle = \sum_{i=1}^{m} p_i D_{zz}^i. \tag{10}$$

If a (x, y, z) rectangular system of coordinates, rigidly bound to the crystal, is selected and a transformation formula for second order tensor components is used on passing from one rectangular system of coordinates to another, we obtain the expression [15]

$$D_{zz}^i = \sum_{k,l = x,y,z} h_k D_{kl}^i h_l. \tag{11}$$

Here h_k, h_l are the directional cosines of the constant magnetic field vector in a (x, y, z) system of coordinates rigidly bound with the crystal. The components D_{kl}^i of the dipole-dipole interaction tensor in (11) are also defined in the (x, y, z) system of coordinates.

As noted above, in the diffusion process, when a water molecule successively takes m permitted places of location (each with the probability p_i) over the time much shorter than the spin-spin relaxation time, local magnetic fields on protons are averaged over all m positions, which leads to the replacement of several doublets in the NMR spectrum by one narrowed doublet.

With regard to (9)-(11), we obtain the following expression describing the orientational dependence of the doublet narrowed as a result of the motion of water molecules

$$2\langle h^{\text{loc}}\rangle = W \sum_{k,l = x,y,z} h_k \langle D_{kl}\rangle h_l, \tag{12}$$

where

$$\langle D_{kl}\rangle = \sum_{i=1}^{m} p_i D_{kl}^i. \tag{13}$$

$\langle D_{kl}\rangle$ is the dipole-dipole interaction tensor averaged over the pathway of a water molecule. Note that the approach proposed

by S. P. Gabuda is also very convenient for the application when it is necessary to average the local field, in particular, in the consideration of the reorientation process and molecular vibrations in crystals.

In the real situation the D_{kl}^{i} tensors in (13) should be preliminary averaged over the vibrational motion of molecules, as shown in [16, 17], because real molecules in the crystale oscillate near the equilibrium position with a frequency of ~10^{12} Hz, which results in the additional averaging of $2h^{\mathrm{loc}}$ splittings.

Unlike (5), in formula (12), when the crystal orientation changes in the external magnetic field, only directional cosines of the constant magnetic field vector change in the (x, y, z) system of coordinates rigidly bound with the crystal. The components of the averaged $\langle D_{kl}\rangle$ tensor do not depend on the orientation of the external magnetic field. This makes it possible to quite simply analyze the effect of the symmetry of the mutual arrangement of **p–p** vectors of the diffusing water molecule unambiguously related to the crystal symmetry on the character of the angular dependence of the narrowed doublet [11, 15].

To each i-th position of a water molecule in the crystal (except the molecules bound by translation or inversion) its own D_{kl}^{i} dipole–dipole interaction tensor corresponds, the tensors corresponding to structurally equivalent molecules being transformed into each other by crystal symmetry operations. The $\langle D_{kl}\rangle$ tensor should reflect the symmetry of the mutual arrangement of fixed positions successively taken by the **p–p** vector during diffusion, and this imposes certain restrictions on it [11, 15].

If the fixed positions **p–p** vector are related by symmetry elements of one of the lowest crystal symmetries (triclinic, monoclinic, orthorhombic), the $\langle D_{kl}\rangle$ tensor is also triaxial in the system of its principal axes, i.e. the systems of coordinates in which nondiagonal elements $\langle D_{kl}\rangle = 0$ for $k \neq l$, the orientational dependence of the doublet splitting has the form

$$2\langle h^{\mathrm{loc}}\rangle = W(\langle D_{xx}\rangle h_x^2 + \langle D_{yy}\rangle h_y^2 + \langle D_{zz}\rangle h_z^2) = \\ = \frac{1}{2}W[(\langle D_{xx}\rangle - \langle D_{yy}\rangle)\sin^2\gamma\cos 2\varphi + \langle D_{zz}\rangle(3\cos^2\gamma - 1)]. \tag{14}$$

It is taken into account that $h_x = \cos\varphi\sin\gamma$; $h_y = \sin\varphi\sin\gamma$, and $h_z = \cos\gamma$; γ and φ are the spherical coordinates of the magnetic field direction H_0.

The $\langle D_{kl}\rangle$ tensor is axially symmetric if the symmetry of positions over which a water molecule diffuses corresponds to the medium crystal symmetry (trigonal, tetragonal, and hexagonal). Here $\langle D_{xx}\rangle = \langle D_{yy}\rangle$, and according to (12)

$$2\langle h^{\mathrm{loc}}\rangle = \frac{1}{2}W\langle D_{zz}\rangle(3\cos^2\gamma - 1). \tag{15}$$

For the cubic symmetry of positions over which a water molecule diffuses, the averaged tensor $\langle D_{kl}\rangle = 0$, which results in a single line in the NMR spectrum for any orientation of the magnetic field

$$2\langle h^{\mathrm{loc}}\rangle = 0. \tag{16}$$

Formula (14) coincides with that proposed in [18] for the reorientation about the twofold axis, and formula (15) coincides with the Gutowsky-Pake formula [12] for the n-fold axis ($n > 2$).

In many cases, the positions of **p–p** vectors taken in the diffusion process are related to all crystal symmetry elements. Situations are possible when this relationship is absent if, e.g., between some positions related by the symmetry elements there is a high potential barrier owing to which this position cannot be taken by a diffusing molecule ($p_i \approx 0$). Thus, the experimental determination of the character of the angular dependence of $2h^{\mathrm{loc}}$ is essential for the elucidation of diffusion ways. On the other hand, experimental values of $\langle D_{zz}\rangle$ and ($\langle D_{yy}\rangle$–$\langle D_{xx}\rangle$) coefficients also bear important information about the arrangement of molecules at their location places, as well as about the amplitude of the vibrational motion. (In this review, $\langle h_{xx}^{\mathrm{loc}}\rangle$, $\langle h_{yy}^{\mathrm{loc}}\rangle$, and $\langle h_{zz}^{\mathrm{loc}}\rangle$ designations are used instead of $\langle D_{zz}\rangle$, $\langle D_{yy}\rangle$, and $\langle D_{xx}\rangle$.)

Formulas (14), (15), and (16) make it possible to obtain expressions describing the shape of the NMR spectrum of a polycrystalline sample with molecular mobility. In [11, 15] it is shown that if the angular dependence of the spectral line position is described by the second order tensor, as it is in the case under study, with the main components

$\langle D_{zz}\rangle \le \langle D_{yy}\rangle \le \langle D_{xx}\rangle$, then the contour of the NMR spectrum of a powder, without taking into account the width of the individual component (δ function) $g(B_c)$, has the form [15]

$$g(B_c)=\begin{cases} 0 & \text{at} \quad B_c \le \frac{1}{2}W\langle D_{zz}\rangle, \\ \frac{1}{\sqrt{\Delta_{xc}\Delta_{yz}}}K\left(\sqrt{\frac{\Delta_{xy}\Delta_{cz}}{\Delta_{xc}\Delta_{yz}}}\right) & \text{at} \quad \frac{1}{2}W\langle D_{zz}\rangle \le B_c \le \frac{1}{2}W\langle D_{yy}\rangle, \\ \frac{1}{\sqrt{\Delta_{cz}\Delta_{xy}}}K\left(\sqrt{\frac{\Delta_{xc}\Delta_{yz}}{\Delta_{cz}\Delta_{xy}}}\right) & \text{at} \quad \frac{1}{2}W\langle D_{yy}\rangle \le B_c \le \frac{1}{2}W\langle D_{xx}\rangle, \\ 0 & \text{at} \quad B_c \ge \frac{1}{2}W\langle D_{xx}\rangle, \end{cases} \tag{17}$$

where $B_c = B - B_0$ is the spectral line position in magnetic field units counted from the resonance field B_0; $\Delta_{kc} = \frac{1}{2}W\langle D_{kk}\rangle - B_c$; $\Delta_{kl} = \frac{1}{2}W(\langle D_{kk}\rangle - \langle D_{ll}\rangle)$; $K(\cdots)$ is the total elliptic intergral.

Fig. 2 shows the NMR spectra of polycrystalline samples containing diffusing water molecules.

Expressions (4)-(17) were used in the works of S. P. Gabuda and his colleagues in the studies of the structural location features, mechanisms of the internal mobility of molecules and their interactions in ionic and molecular crystals [19-32], in minerals [33-57], at phase transformations in crystals [58-69], and also hydrated proteins [70-78] and catalysts [79-81]. It is worth noting that formulas (4)-(17) can be used not only for the analysis of the diffusion mobility of water molecules and also for some other molecules characterized by pronounced intramolecular dipole-dipole interactions of nuclear magnetic moments forming doublet splittings. In particular, the diffusion (self-diffusion) of HF, NH_3, and BrF_3 molecules [30, 82-84], *n*-paraffines [80], C_6H_6 and $C_6H_3BrCl_2$ [81, 85], $(NH_2)_2CNH$ [22], $(H_3C)_2NCHO$ and $(H_3C)_2CO$ [86, 87] was studied. A detailed description of the proposed model and its further development are presented in a number of original articles mentioned in this review and monographs [8, 13, 14, 88, 89].

Below we analyze some works of Prof. S. P. Gabuda, which reveal that his model is promising for the investigation of structural and dynamic properties and also phase transitions in various objects, including biological. Note that the state of

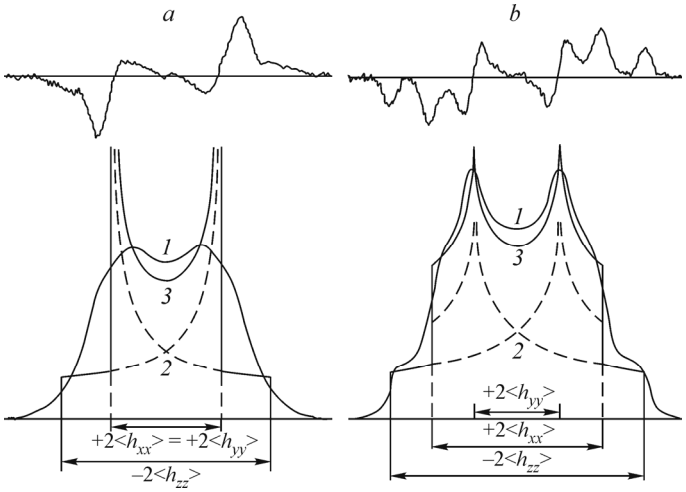

Fig. 2. ^{1}H NMR spectra (at the bottom, absorption; at the top, first derivatives of the absorption spectrum): axially symmetric averaged local magnetic field (η = 0) (*a*); triaxial averaged local magnetic field (η = 0.33) (*b*). Experimental absorption line (*1*) and theoretically calculated curves (*2*), and their sum (*3*), corresponding to formulas (14) and (15).

water molecules diffusing over the structural positions of crystals S. P. Gabuda lately defined as the state of a nanofluid under the conditions of quantum limitation.

AVERAGING OF LOCAL MAGNETIC FIELDS IN HYDRATED SYSTEMS

Crystal hydrates and minerals

Hydrated ferroelectrics. The historically first ferroelectric, which was turned to be the $KNaC_4H_4O_6{\cdot}4H_2O$ compound (Rochelle salt), contains crystallization water. I. V. Kurchatov (1933) associated the appearance of spontaneous polarization with the ordering of H_2O dipole moments, however, the existing research methods have not been able to establish the presence of the corresponding molecular mobility in both paraelectric state and ferroelectric phase. Moreover, the structure studies of other ferroelectrics discovered later have shown that in the majority of cases, the appearance of spontaneous polarization is accompanied by a change in the positions of all atoms in the structure, more often not containing water at all. Therefore, the theories of ferroelectrics with rotating dipole molecules gave place to more adequate ones, however, among numerous ferroelectrics a family of crystal hydrates was found, in which, according to ^{1}H NMR data, water molecules were mobile, and the model of ordering dipole moments was applicable [19-24, 27-29]. For instance, the properties of ferroelectrics of the potassium ferrocyanide family $K_4M(CN)_6{\cdot}3H_2O$ (M = Fe, Mn, Ru, and Os) are determined by the ordering of dipole moments of water molecules [8, 19, 27-29]. The determination of the directions of **p–p** vectors from the NMR data and the analysis of the diffusion process of water molecules made it possible to unambiguously establish the system of dipole moments and to predict (found in further experiments) the direction of spontaneous polarization. It is shown that the ferroelectric behavior of $K_4Fe(CN)_6{\cdot}3H_2O$ can be associated with a system of dipole moments of one of the two structurally inequivalent types of H_2O molecules.

Another type of ferroelectrics is considered on the example of colemanite and guanidine aluminum sulfate. It is shown that in the first case, the role of the trigger is played by a water molecule [4], and in the second case, by $[C(NH_2)_3]^+$ guanidonium ions [22]. The displacements of trigger groups, resulting in the repolarization of crystals have been studied in detail.

NMR analysis of water in beryl. One of the characteristic features of mineral beryl with the idealized formula $Al_2Be_3Si_6O_{18}{\cdot}xH_2O$ is the systematic presence of variable amounts (x) of water molecules in its composition, and their content can reach three weight percent or nearly one molecule per formula unit. Data on the particular location of water and the bonding in the crystal structure of beryl (and isotypical cordierite) have still been under discussion.

In the ^{1}H NMR study (Fig. 3) of four beryl samples with different chemical compositions it is shown that the structure can contain three structurally inequivalent water molecules whose proton-proton vectors are: a) perpendicular to the sixfold axis $-(H_2O)_I$; b) parallel to it $-(H_2O)_{II}$, and c) oriented at an angle of ~60° to it $-(H_2O)_{III}$; there are also isolated protons in the form of H^+ or OH^- [44]. Three structurally inequivalent types of water molecules are seen from the NMR spectra of beryl single crystals measured at 77 K. Each spectrum contains three spectra of water molecules with different splittings $2\langle h^{loc}\rangle$ (Fig. 3). The features of ^{1}H NMR spectra measured at room temperature indicate the reorientation of $(H_2O)_I$ molecule about the ***c*** axis and the exchange (diffusion) between $(H_2O)_{II}$ and $(H_2O)_{III}$. Quantitative ratios of the revealed types of water in beryls depend on their chemical composition (Fig. 3).

The ^{1}H NMR analysis of water in beryl is a bright example of the application of model (4) for the determination of the orientation of water molecules in crystal hydrates. Only the occurrence of either third type of water $(H_2O)_{III}$ or OH^- groups can generate some discussion [44].

Character of mobility of water molecules in desmine. Desmine (stilbite) $Na_2Ca_4[Al_{10}Si_{26}O_{72}]{\cdot}28H_2O$ is a mineral from the family of layered zeolites, symmetry space group $C2/m$, monoclinic cell parameters $a = 13.64$ Å, $b = 18.24$ Å, $c = 11.27$ Å, $\beta = 128°$. Using the NMR method, in [43] a natural desmine crystal was studied during its rotation about three mutually perpendicular axes X, Y, Z, the X and Y axes coinciding with the a and b axes, and $Z = c\sin\beta$. Orientational dependences of the positions of doublet components at 77 K are described by the Pake formula [4]. From the analysis of the

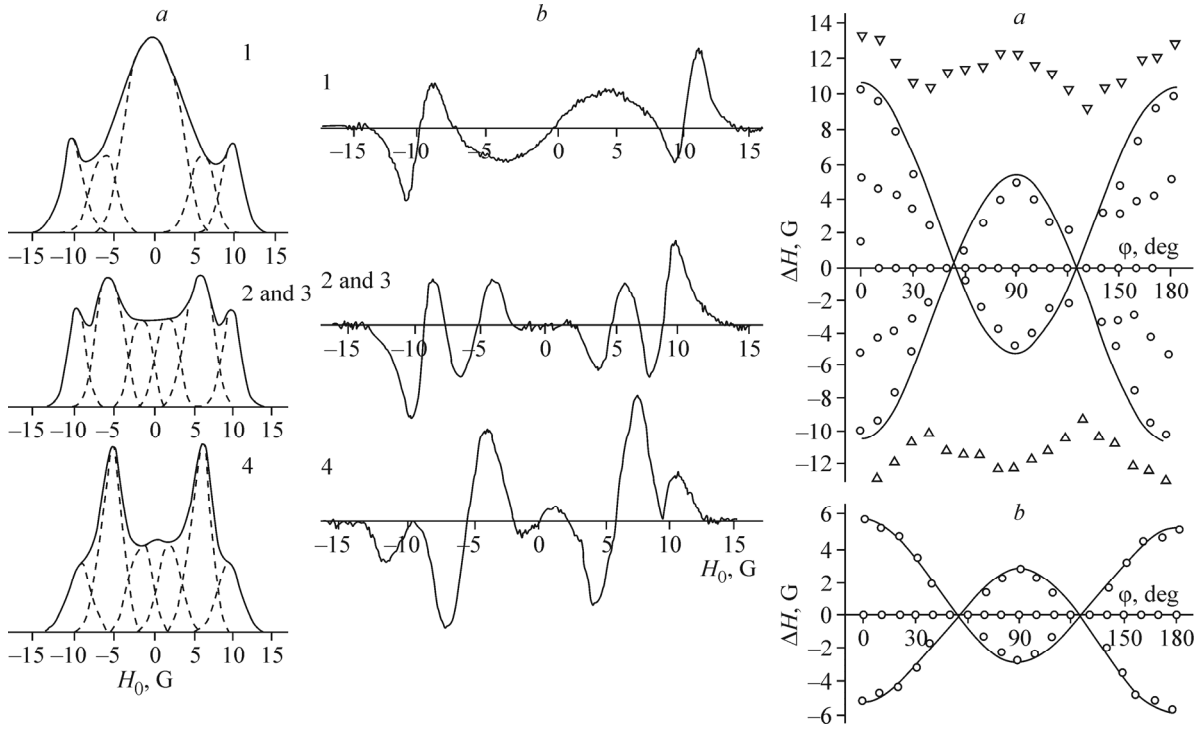

Fig. 3. [1]H NMR spectra of beryl single crystals: absorption lines (*a*) and first derivatives of absorption lines (*b*) at 77 K (left). Angular dependences of doublet splittings (circles) and total widths (triangles) in the spectra of beryl single crystals during their rotation about the [100] axis: at 77 K (solid line is drawn according to the Pake equation [4]) (*a*); at 293 K (solid curve is drawn according to transformed equation (4): $\Delta H = \frac{3}{2}\mu r^{-3}(3\cos^2\delta\cdot\cos^2\varphi - 1)$ at $\delta = 0^i$ (*b*). 1-4 are the numbers of beryl samples with different compositions [see in 44].

[1]H NMR spectra (the values of splittings between the components and their intensities, Fig. 4) measured at 77 K it was found that in desmine $p_1 = 3/7$ of all **p–p** vectors were oriented parallel to the [001] direction, $p_2 = 3/7$ parallel to [010], and $p_3 = 1/7$ at angles of ±55° to the [100] direction in the (001) plane. With an increase in the temperature the NMR spectra transform and above 250 K the NMR spectrum is characterized by one doublet splitting $2\langle h^{loc}\rangle$ (Fig. 4).

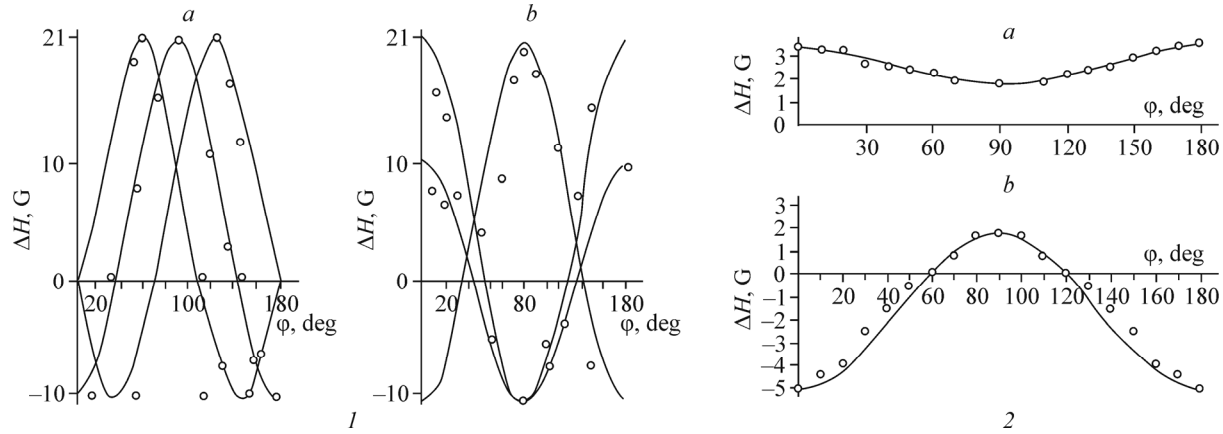

Fig. 4. Angular dependences of doublet splittings ΔH of [1]H NMR spectra of desmine at 77 K. (*1*): rotation about the *X* axis (angles are counted from the *Z* axis) (*a*), rotation about the *Z* axis (angles are counted from the *Y* axis) (*b*). Angular dependences of the doublet splittings $2\langle h^{loc}\rangle$ in the [1]H NMR spectra of desmine at 290 K (*2*): crystal is rotated about the *Z* axis (angles are counted from the *Y* axis) (*a*), crystal is rotated about the *Y* axis (angles are counted from the *Z* axis) (*b*). Solid line is the dependence calculated by equation (4).

Results of the calculation with an accuracy up to the constant factor coincide with the experimental data obtained at room temperature in [6]. A theoretical value of $3/2\mu R^{-3} \approx 1.5$ G calculated by formulas (4) and (5) is larger than the experimental one of ~0.85 G. The reason for the difference is due to the contribution of excess vibrations [90]. Expression (4) describes well the high temperature angular dependence of $2\langle h^{loc}\rangle$ when the geometric characteristics of **p–p** vectors, obtained at 77 K, are used. From here it follows that the temperature changes in the spectra of desmine at temperatures above 200 K are explained by the translational diffusion of water molecules over the regular lattice sites in each of which the arrangement of **p–p** vectors coincides with the arrangement found at 77 K.

Character of the mobility of water molecules in heulandite and clinoptilolite. Heulandite $NaCa_4(Si_{27}Al_9)O_{72}\cdot 24H_2O$ is zeolite, symmetry space group $C2/m$, monoclinic cell parameter $a = 7.44$ Å, $b = 16.84$ Å, $c = 15.88$ Å, $\beta = 91.4°$. Experimental NMR spectra [16] at 77 K show that in the structure of this crystal 2/5(p_1) of all **p–p** vectors are oriented parallel to [010], 2/5(p_2) lie in the (001) plane at angles of ±35° to [010], and 1/5(p_3) lie in the (001) plane at angles of ±55° to the [010] direction. The angular part of expression (4), calculated with the presented parameters p_i and orientation angles of **p–p** vectors completely coincides with the experimental high-temperature angular dependence of $2\langle h^{loc}\rangle$ and is axially symmetric ($\eta = 0$) with the [010] symmetry axis. This seems to not correspond to either crystal morphology or its structure with the monoclinic cell. However, as the analysis shows, the axial symmetry of $2\langle h^{loc}\rangle$ is a random consequence of the specific arrangement of water molecules in this structure and an additional mechanism of averaging local magnetic fields due to librational vibrations [16, 90].

Later, in the study of single crystal samples of clinoptilolite $Na_2K_2Ca[Al_6Si_{30}O_{72}]\cdot 22H_2O$ and heulandite $Ca_3Mg[Al_8Si_{28}O_{72}]\cdot 24H_2O$, which are characterized by the same topological type of alumosilicon-oxygen frameworks and the symmetry space group $C2/m$, but have another Al/Si ratio and another composition of outer-framework exchange cations, it is shown that at temperatures below 170 K a fixed distribution of H_2O over the structural positions, but different for these two minerals and the previous heulandite sample, is observed. However, at high temperatures (Fig. 5) the obtained experimental dependences almost do not differ for two crystals; the degree of deviation of the angular dependences from the uniaxial or axial symmetry is relatively small. For heulandite its value is $\eta = (\Delta B[001] - \Delta B[100])/\Delta B[010] \approx 0.05$, for clinoptilolite the degree of non-axiality $\eta = (\Delta B[001] - \Delta B[100])/\Delta B[010]$ is ~0.15. Thus, from the nearly axial symmetry of the angular dependence of the NMR spectra of the high-temperature phase of the system under study the conclusion follows about practically isotropic reorientation of water molecules in eightfold positions located on two sides of the (010) planes in heulandite (fourfold in clinoptilolite), which play the role of bridges between the exchange cations and oxygen atoms located in (010) planes of the $(Si,Al)O_4$ framework. The obtained result indicates that the dipole moment of water molecules is somewhat "unfrozen" above 270 K. Note that this is one of the conditions for the appearance of the effect of microwave absorption in both heulandite and clinoptilolite [57].

Character of the mobility of water molecules in natrolite. Natrolite $Na_2[Al_2Si_3O_{10}]\cdot 2H_2O$ is zeolite, symmetry space group $Fdd2$, orthorhombic cell parameters $a_0 = 18.3$ Å, $b_0 = 18.6$ Å, $c_0 = 6.57$ Å, however, the averaged local magnetic fields in it not only do not correspond to the triaxial ellipsoid but even are averaged practically to zero. The reason for this is

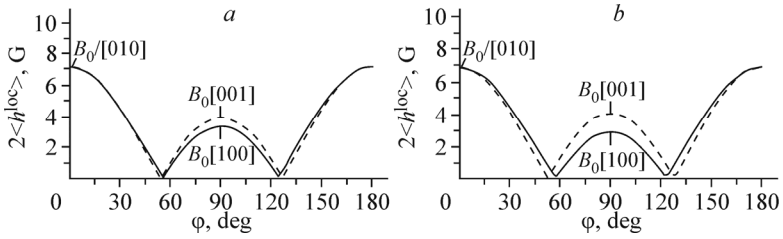

Fig. 5. Angular dependences of doublet splittings in the ^1H NMR spectra of heulandite (290 K) (*a*) and clinoptilolite (290 K) (*b*), obtained on rotation of smaples about the [100] (dashed lines) and [001] axes (solid curves). B_0 is the external magnetic field.

revelaed in the study of the arrangement of water molecules. It is found that the **p–p** vectors of water molecules in natrolite are located in (110) and ($\bar{1}\,\bar{1}$0) planes at angles of ±35° to the (001) plane. From here it follows that the angle between the **p–p** vectors of all water molecules and the ***c*** axis of the structure is close to the magic angle (54°44′), and hence, at diffusion the averaging of $\langle h^{loc}\rangle$ almost to zero is inevitable [33, 37, 53].

Thus, the symmetry of the $\langle h^{loc}\rangle$ tensor on the protons of diffusing water molecules reflects the crystal symmetry. Only some specific cases related to the features of the arrangement of **p–p** vectors with respect to the external magnetic field are possible.

Hydrate layers of clay minerals

The real structure of water layers in clay minerals is more compex [91] for the methods and approaches used in the study of crystal hydrates and zeolites to be employed. For instance, water layers between the silicate layers of montmorillonite $\{Al_4[Si_8O_{20}](OH)_4{\cdot}nH_2O\}$ contain one- and two-charged cations. The X-ray crystallographic analysis of the successive stages of montmorillonite hydration $\{Al_4[Si_8O_{20}](OH)_4{\cdot}nH_2O\}$, which were traced by the value of the ***c*** parameter (perpendicular to the layer plane) gives evidence that between the silicate layers there can be 0, 1, 2, 3, 4, and more layrs of water molecules. Water molecules in the layers form a hexagonal packing; they are hydrogen bonded between themselves and the surface of silicate groups.

Therefore, for clay minerals a general scheme was proposed for the positions of water molecules: T positions in which water molecules are characterized by a tetrahedral coordination with other water molecules by analogy with the positions of water molecules in ice, and these positions must be if there are several layers of water molecules between the silicate layers; S^+ and S^- are the surface positions created by oxygen atoms or hydroxyl on the surface of clay silicate layers for the coordination of water molecules to them; C are the positions in the sphere of cations in the clay composition; I are the positions for water in spacious interstices. According to equation (4), at the diffusion of water molecules the averaged local magnetic field should have the form

$$\langle h^{loc}\rangle = p_1\langle h(T)\rangle + p_2\langle h(S^+)\rangle + p_3\langle h(S^-)\rangle + p_4\langle h(C)\rangle + p_5\langle h(I)\rangle, \quad (18)$$

where p_1, p_2, p_3, p_4, and p_5 are the probabilities of the occupation of positions T, S^+, S^-, C, and I at $p_1 + p_2 + p_3 + p_4 + p_5 = 1$. As the general analysis of the features of positions T, S^+, S^-, C, and I shows, $\langle h^{loc}\rangle$ is determined only by the mobility of water molecules in positions S^+ and S^-; the contribution of the others results in $\langle h^{loc}\rangle = 0$.

Fig. 6 depicts possible coordinations of water molecules to positions S^+ and S^-. If fluoro derivatives of clay minerals are considered, then the contribution to $\langle h^{loc}\rangle$ from the positions of water molecules in S^+, which are bound to hydroxyl, is

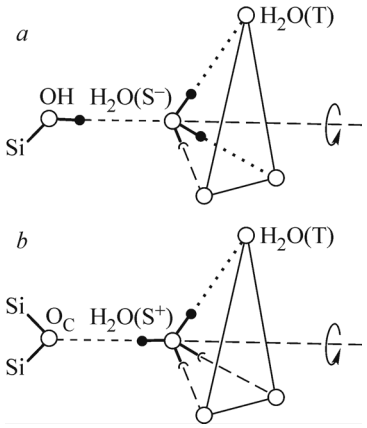

Fig. 6. Arrangement scheme of water molecules: adsorbed on the surface center of the S^- type (OH group) (*a*); adsorbed on the surface center of the S^+ type (O^{2-} ion) (*b*).

absent. However, fluorine atoms as well as oxygen atoms are acceptors of the water H bonds and all S^+ positions can be replaced by S^- positions.

In the S^- position, during the reorientation of water molecules in this position the **p–p** vector always remains parallel to the arrangement plane of the hydrate layer. In the case of water molecules located in the S^+ positions, one of the molecular protons is constantly orieneted towards the oxygen atom of the silicate layer, forming the H bond of water molecules with the framework.

If the orientation of **p–p** vectors of water molecules in S^+ and S^- positions is taken into account, then the NMR spectra must be presented by narrow doublets:

for montmorillonites and vermiculites in the OH-form

$$2\langle h^{loc}\rangle = 5.25 \text{ G } (p_2 - p_3)(3\cos^2\theta - 1), \tag{19}$$

for fluoromontmorillonites and fluorovermiculites

$$2\langle h^{loc}\rangle = 5.25 \text{ G } (p_2 + p_3)(3\cos^2\theta - 1), \tag{20}$$

where θ is the angle between the magnetic field direction and the normal to the plane of the clay mineral layer. From here it is seen that for fluorinated clay minerals larger doublet splittings of $2\langle h^{loc}\rangle$ could be expected than for their analogues of OH-forms.

Proposed model (18)-(20) for the diffusion of water molecules in the interlayer space of clay minerals is able to correctly predict the character of the angular dependence of doublet splittings, splitting values, and their temperature dependence and makes a substantial contribution to the comprehension of the structure of hydrate layers in clays [8]. The applicability of the model is obviously proved by the character of changes in the doublet splittings of $2\langle h^{loc}\rangle$ in the measurement of ^{1}H NMR spectra of clay minerals and their fluorinated analogues: the spectral half-width of the sodium form is 2.9 G and of calcium one >0.5 G (the splitting is not observed) [92]. For the fluorinated analogues the ^{1}H NMR spectra have a well-resolved structure and the maximum splitting at the magnetic field orientation perpendicular to the layer plane is ~9 G (sodium form) and ~3 G (calcium form) [93], as is also shown by formulas (18)-(20).

The other authors interpreted the NMR data of diverse clay minerals in terms of the anisotropic rotation of water molecules, precession angles were determined, and so on [93, 94]. Note that for the accurate calculation of $\langle h^{loc}\rangle$ values on the protons of water molecules data on the nature of centers holding water molecules in the interlayer space are needed, therefore model (18) for the characterization of ^{1}H NMR spectra can provide important information for the refinement of the strauctures of adsorption surfaces.

Hydrate shells of collagen type proteins

Fibrous protein collagen composes approximately one-third of all polypeptides in human and animal organisms [95]. In tendons the collagen content reaches 94%, in skin it is 75%, and in the bone it is about 50%. The collagen is characterized by a high degree of molecular ordering and crystallicity. The main structural unit of the collagen is rod-like tropocollagen molecules with a length of ~2800 Å and a diamtere of ~14 Å. The tropocollagen molecule is a triple helix consisting of three non-identical polypeptide chains, each of which consisting of approximately 1040 amino acid residues. It is shown [96] that the collagen structure is formed by the parallel packing of tripeptide tropocollagen molecules with a longitudinal shift by ~1/4 of their length. In the longitudinal direction (the *c* axis of the collagen structure) the terminal C and N groups of the neighboring three-helical molecules do not contact and the spaces or slits are about 340 Å long. The distribution of similar vacancies with a cross-section of about 15 Å in the supramolecular structure of collagen is strictly ordered, which is manifested in the form of the characteristic transverse striation of collagen fibers with the period c_0 = 640 Å, which is visible in electron microscopic images [96-98]. The composition of native (undamaged) collagen contains bound water amounting to about 2/3 (or ~66%) of the total tendon mass.

In accordance with the above, the diffusion model is based on the assumption that all water in collagen practically does not change in its properties from free one whose structure is derived from the structure of disordered ice. The exception is only some water molecules in the frontier single layer between the protein surface and the surrounding aqueous solution. For the molecules of this layer a sufficiently rigid bond, first of all, with the active centers of polypeptide allowing only

exchange processes with molecules in the hydrate shell bulk, is expected. The diffusion of water molecules over all positions in both bulk and surface averages h^{loc}

$$\langle h^{loc}\rangle = p_1\langle h(T)\rangle + p_2\langle h(S^+)\rangle + p_3\langle h(S^-)\rangle + p_5\langle h(I)\rangle, \quad (21)$$

where p_1, p_2, p_3, and p_4 are the occupancy probabilities of T, S^+, S^-, and I positions at $p_1 + p_2 + p_3 + p_4 = 1$, as well as for clay minerals, the S^+ and S^- positions of water molecules being near the groups containing oxygen and nitrogen atoms on the surface of protein molecules. The theory of the anisotropic rotation of water molecules [99], which has been repeatedly suggested not only for the interpretation of the NMR spectra of water in collagen but also crystal hydrates, clays, and zeolites was alternative to this model. According to this model, all water molecules are identical in the system and behave similarly to molecules in liquid crystals in which the molecules mainly rotate about the axis fixed in space. It should be noted that in biological tissues diverse chemico-biological reactions affecting the local magnetic fields are possible, and diffusion model (4) and (21) of the motion of water molecules can be suppressed, however, there can be the diffusion of molecules.

As further investigations have shown, model (4) with regard to (21) was supported in [75-77], where it was shown that the structure of one part of bound water in disordered regions of the collagen protein structure belongs to the tectohydrate type, involving a continuous three-dimensional framework of water molecules with a tetrahedral coordination characteristic of ice and clathrate hydrates (Fig. 7). The properties of another part of bound water are close to the properties of water in zeolites.

The significance of the results of NMR studies is due to the role of the considered object (collagen) in biology and medicine because collagen comprises one third of all proteins in the organism. There are so-called collagen diseases (Alzheimer's disease, senile changes in skin, etc.) for which the molecular mechanisms have been unclear so far. The developed approaches can be useful for the structural visualization of some stages of pathology appearance and the clarification of possible counteractions.

PHASE TRANSITIONS IN GUEST SUBSYSTEMS OF ZEOLITES

Another application of model (4) proved to be efficient for the detection and analysis of phase transitions in the subsystems of guest molecules in framework structures under various external conditions [55, 58-69]. Formula (4) shows that

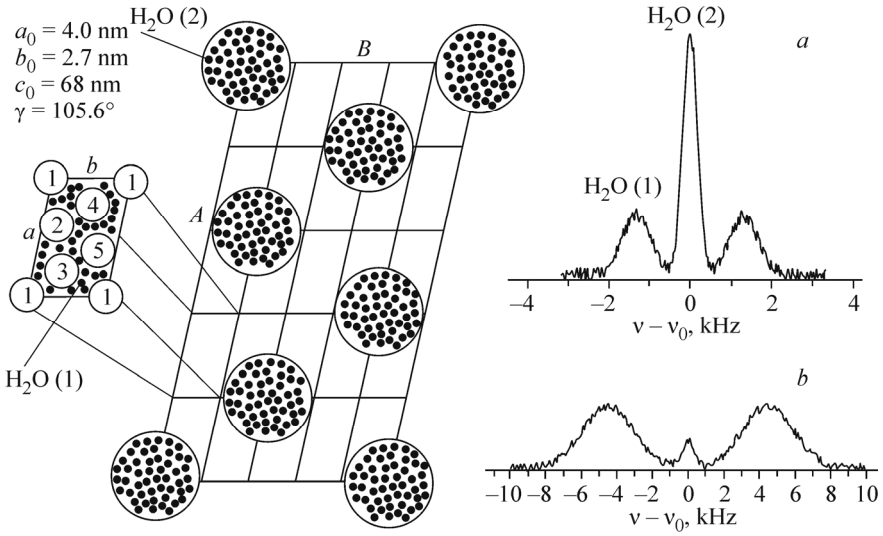

Fig. 7. Collagen structure in projection along the axis of channels formed by the parallel packing of tripeptide molecules; the collagen unit cell falls into a sequence of dense (with a length of 0.46 c_0) and loose (0.54 c_0) parts. In the first parts the nanotube width is about 0.7-1.0 nm, and in the second part it is ~3.5 nm; nanotubes are filled with a fluid (water) (left). ^{2}H NMR spectra of two types of water at +20°C (*a*). At –10°C H_2O subsystem (2) freezes out (*b*) (right).

structural transformations associated with the appearance/disappearance of structural positions (their number, structure type, and also crystal symmetry) should cause certain changes in the characteristics of $\langle h^{loc} \rangle$. In the general case, changes can be found for all components of the ellipsoid of averaged local fields $\langle h^{loc} \rangle$ ($\langle h_{xx}^{loc} \rangle$; $\langle h_{yy}^{loc} \rangle$ and $\langle h_{zz}^{loc} \rangle$) because $\mathrm{Sp}\langle h_{kl} \rangle = 0$. Thus, by studying the dependences of $\langle h_{ii}^{loc} \rangle$, e.g., on the temperature, pressure, or concentration of molecules in porous substances it is possible to discover structural changes in molecular guest subsystems.

Phase transitions in chabasite

The crystal structure of natural zeolite $Ca_2[Al_4Si_8O_{24}]\cdot nH_2O$ (chabasite) is formed by the interlocking of double six-membered rings of the composition $[(Al_2Si_4O_{12})_2]^{4-}$, forming a rigid three-dimensional alumosilicon-oxygen framework with the space group $R\bar{3}m$ and lattice parameters $a = 9.40$ Å, $\alpha = 94°15'$. In large cavities of the completely hydrated structure there are $[2Ca(H_2O)_5\cdot 3H_2O]^{4+}$ groups, and in them calcium ions enter into the composition of aqua complexes. In completely dehydrated chabasite, Ca^{2+} ions are located in the centers of six-membered rings playing the role of traps for calcium ions and other cations substituting for calcium in ion exchange reactions. In the studies chabasite specimens from basalt of the deposit on the Khilok River, Transbaikalia (Russia) were used. The averaged chemical composition of the specimens corresponds to the formula (in the calculation per unit cell): $(Na_{0.24}K_{0.10}Ca_{1.65})[Al_{3.79}Si_{8.25}O_{24}]\cdot nH_2O$ ($n = 12.8$).

By the ^{1}H NMR method the dependence of the *zz* component of the local magnetic field on the nuclei of hydrogen atoms of water molecules on their concentration $1.5 \le n \le 12.8$ (n is the number of H_2O molecules in the unit cell) was studied [67, 68]. It is shown that at $n > 1.8$ water molecules take part only in the circular diffusion near Ca^{2+} ions located in six-membered alumosilicate rings of the structure, and at $n > 1.8$ the translational diffusion of H_2O is observed. A change in the character of the mobility is attributed to the release of a part of exchange Ca^{2+} cations from ionic traps and to the formation of $[Ca(OH_2)_x]^{2+}$ aqua cations in zeolite cavities. The bimodal character of the location of water molecules and Ca^{2+} ions takes place within the water content variation from $n \approx 2$ to $n \approx 8.5$. At $n = 8.55$ there is a concentration phase transition due to ordering of the structure of the guest subsystem in the form of $[Ca(OH_2)_4]^{2+}$ aqua complexes. A similar transition at $n = 10.25$ is caused by the formation of $[Ca(OH_2)_5]^{2+}$ complexes. Both transitions are accompanied by thermal effects (Fig. 8).

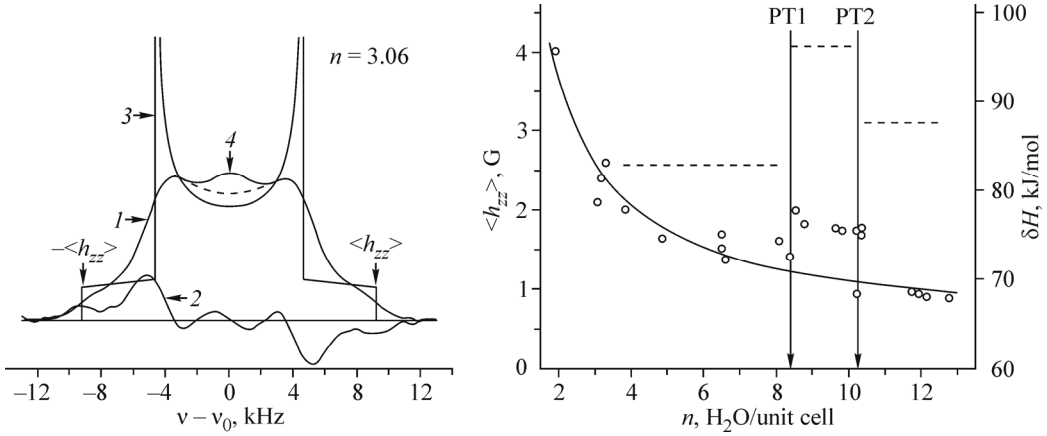

Fig. 8. ^{1}H NMR absorption spectrum (*1*) and the first derivative (spectrum (*2*)) of partially dehydrated chabasite; calculated ^{1}H NMR spectrum (*3*); central line bound with acid centers (*4*) (left). Dependence of the order parameter $\langle h_{zz} \rangle$ on the water content in channels (○); the solid line is the calculated $\langle h_{zz} \rangle$ dependence on n; dotted lines are the data of the calorimetric study of the hydration heat δH of partially dehydrated chabasite samples. Arrows indicate the structural phase transitions related to the water subsystem (right).

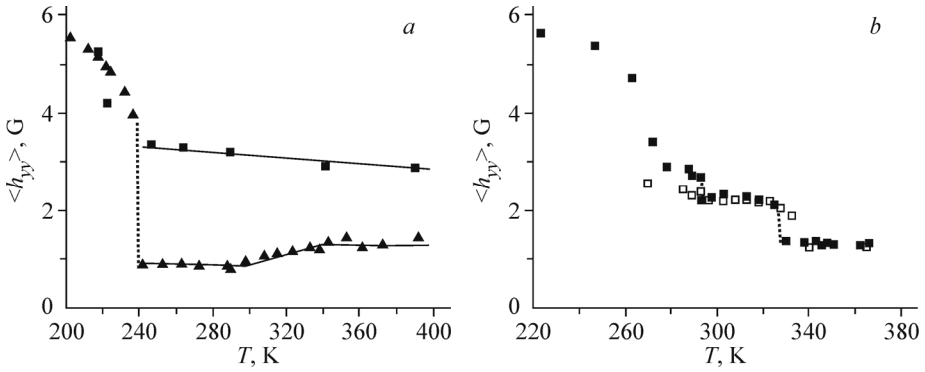

Fig. 9. Temperature dependence of the *yy* component of the local magnetic field $\langle h_{yy} \rangle$: for leonhardite samples at $n = 10.8$ (■) and $n = 14.4$ (▲) (*a*); for laumontite samples at $n = 18$ (■) and $n = 16$ (□) (*b*). Vertical lines show the phase transitions.

The obtained results about the concentration phase transitions in chabasite give evidence in favor of the model of a stepwise discrete character of the occupation of zeolite pores by water molecules, which may be associated with the existence of some series of stable forms of aqua complexes of exchange cations.

Phase transitions in laumontite and leonhardite

Laumontite and leonhardite are zeolites of the analcime group and represent two differently hydrated modifications with the same chemical composition $Ca_4[Al_8Si_{16}O_{48}]\cdot nH_2O$, space group *C*2/*m*, unit cell parameters $a = 14.90$ Å, $b = 13.17$ Å, $c = 7.55$ Å, $\beta = 111.5°$. For the study a single crystal and polycrystalline samples of laumontite from the deposit on the Nidym River (Russia) were used. The averaged chemical composition of the samples corresponds to the formula (in the calculation per unit cell): $(Na_{0.23}K_{0.06}Ca_{3.85})[Al_{7.96}Si_{16.03}O_{48}]\cdot nH_2O$. By the ^{1}H NMR method the dependence of the *yy* component of the local magnetic field ($\langle h_{yy} \rangle$) on the nuclei of hydrogen atoms of water molecules on their concentration $10 \le n \le 18$ (*n* is the number of H_2O molecules in the unit cell) was studied. A seies of phase transitions was found in both samples (Fig. 9).

The structural transformation leonhardite ↔ laumontite was detected at $n \approx 14.4$. Structural data for leonhardite (at $n \approx 12$) show that water molecules enter into the composition of $[Ca(OH_2)_3]^{2+}$groups. With an increase in the water content (to $n \approx 13.2$-14) additional water molecules locate in the space between the mentioned island groups, forming hydrogen bridges of H_2O–H_2O bonds with them. Here the competition of H_2O–H_2O hydrogen bonds (guest–guest interactions) with ion-dipole interactions in $[Ca(OH_2)_3]^{2+}$ groups (which can be assigned to guest–host interactions) results in disordering [38, 63]. At further saturation of the system with water up to $n \approx 18$ a new, partially ordered under normal conditions the sublattice of water molecules appears in the laumontite structure. Similar behavior can be related to a relatively gret freedom of the arrangement of water molecules in wide channels of the structure. In this structure of the system the main role in the arrangement of water molecules is played by the ratio of guest–host and guest–guest coupling strengths and its variation with a change in the water content. Vibrations of molecules in such a system cannot be already represented by the model of independent oscillators. A mathematical consideration of systems of coupled oscillators [100] shows that with a smooth increase in the coupling strengths between the oscillators (for the case of the channel system due to an increase in the water content) the chaotic behavior of guest particles and their disordering can appear abruptly. The incorporation of additional molecules and an increase in the coupling strengths between them can result in modulation and partially ordered structures, however, the disorder of the structure is the main feature of this system [100]. The model described resembles the behavior of molecules in the guest subsystem in laumontite and most likely can also be used for the interpretation of structural rearrangements in other wide-pore channel systems.

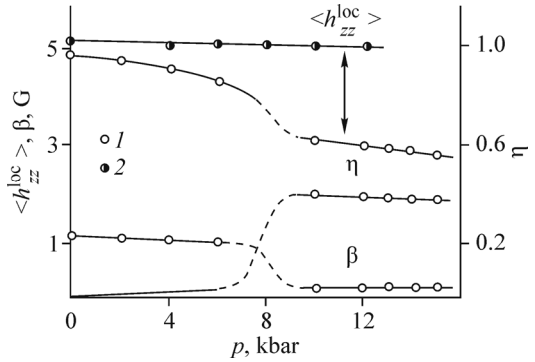

Fig. 10. Dependences of the $\langle h_{zz}^{loc} \rangle$, η, and β parameters of the ^{1}H NMR spectra of natrolite on the pressure in the penetrating (*1*) and non-penetrating (*2*) media. In the phase transition region (dashed lines) parameters were not determined.

Phase transitions in natrolite and edingtonite at high pressures

Of special interest are the works on the study of the mobility of water molecules in zeolites when water penetrates into a sample under pressure. For natrolite the dependences of the parameters of NMR spectra ($\langle h^{loc} \rangle$, η, and the broadening parameter of the spectral component β) measured by the procedure developed in [8, 10, 15] are shown in Fig. 10. Polycrystalline samples of natrolite were placed in a fluoroplastic ampoule into which the fluid penetrating (H_2O) or not penetrating ($(C_4F_9)_2O$) into zeolite was poured. An abrupt change in the parameters at 7-8 kbar gives evidence of the phase transition due to an increase in the water content in natrolite [60]. This experiment is the first example of the phenomenon of crystal swelling. A large η indicates that the symmetry of the high-pressure natrolite phase is no lower than orthorhombic. It is found that the correlation frequency (the frequency of jumps of water molecules per time unit, which was found the parameter β) increases with an increase in pressure. This fact is explained based on the assumption that in the initial lattice of a dry sample of natural natrolite there are empty interstices (additional positions with the occupation probability p_i) occupied by water molecules only under pressure. In this case, not only structural positions for water molecules in natrolite but also interstices occupied only under pressure are involved in the diffusion process [33, 50, 55, 60].

The found increase in the molecular mobility at high pressures must play an additional role in the transfer phenomena in molecular pores and channels of rocks and in Earth's depths, also at high temperatures.

NH_3–H_2O *interactions in zeolite pores. In situ* ^{1}H NMR

The interaction between NH_3 ammonium molecules and H_2O water in zeolite pores was studied by the *in situ* ^{1}H NMR method [65, 69]. Powders and single crystal samples of natural zeolites (heulandite $Ca_4[Al_8Si_{28}O_{72}]\cdot nH_2O$ and clinoptilolite $(Na,K,Ca_{1/2})_6$ $[Al_6Si_{30}O_{72}]\cdot nH_2O$), where *n* is the number of water molecules, were used as model systems. The interpretation of the spectra was based on model (*4*) and the atlas of ^{1}H NMR spectra of ion-exchange forms of clinoptilolite and heulandite tuffs. It is shown that the subsystem of water molecules in zeolite pores actively absorbs NH_3 from the gas phase and the penetration of NH_3 molecule into zeolite pores is accompanied by the disordering of the hydrogen sublattice of zeolite water and rapid proton exchange $NH_3 + H_2O \leftrightarrow [NH_4]^+ + [OH]^-$ with the characteristic correlation frequency $\nu_c \approx 40$ kHz (Fig. 11). The reaction of the system to NH_3 is most rapid for Na-clinoptilolite with the ratio Si/Al = 5 and the slowest reaction is for Ca-heulandite with the ratio Si/Al = 2.8 (Fig. 12). Another reaction of the interaction between NH_3 ammonium molecules and H_2O water in zeolite pores is presented by the interaction of $[NH_4]^+$ with exchange Na^+ and Ca^{2+}

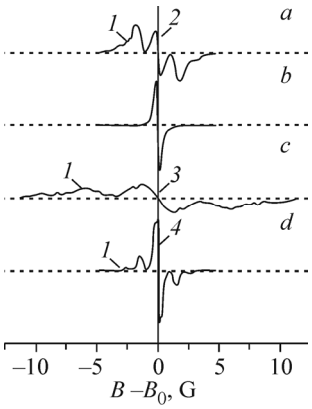

Fig. 11. Transformation of ^{1}H NMR spectra (first derivatives of absorption spectra) in clinoptilolite tuff in the ammonia vapor atmosphere (73 Hg mm): initial sample, $T = 290$ K (*a*); $T = 290$ K, exposition time $t = 30$ h (*b*); $T = 200$ K, $t = 30$ h (*c*); $T = 290$ K, NH_4 ion-exchange form of clinoptilolite (*d*); signal from water molecules in zeolite (*1*), signal of water molecules in montmorillonite (*2*), signal from the NH_3 group (*3*), signal from NH_4^+-group (*4*).

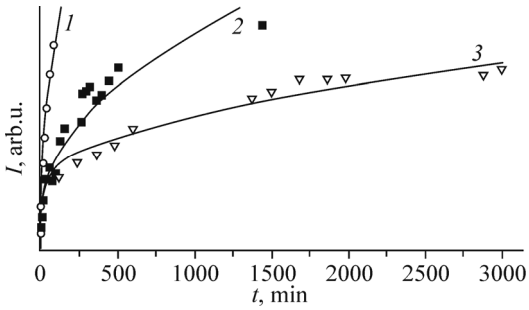

Fig. 12. Switch-on kinetics of the mechanism of the fast proton exchange in zeolite water under the effect of NH_3: Na-form of clinoptilolite (*1*), Cs-form of clinoptilolite (*2*), Ca-form of heulandite (*3*). *I* – proportional to the Lorentz line intensity (Fig. 11*b*).

cations of the zeolite structure. Slow ion exchange $[NH_4]^+ \rightarrow [Na,Ca_{1/2}]^+$ and the binding of $[NH_4]^+$ in cationic positions and also the abrupt release of (Na,Ca $Ca_{1/2}$)OH from the pores to the external surface of zeolite grains were visualized by means of ^{1}H NMR (Fig. 11). Later it was confirmed by Bulgarian scientists (D. G. Kirov and L. G. Filizova).

MOBILITY OF HYDROGEN ATOMS

Thermal vibrations

Numerous experiments confirm the validity of model (*4*), however, there are remarks reduced to that they do not take into account vibrations of nuclei, i.e. small variations of R near the equilibrium value R_0 and the θ angle near some equilibrium θ_0. A similar remark is also referred to the Pake formula [4]. According to neutron diffraction data, in H_2O molecules in crystal hydrates the interproton distance $R_0 = 1.52$ Å, which is close to the R_0 value in water vapor. Hence, the maximum value of the local magnetic field not averaged by diffusion $2h^{loc} = 24.2$ G. The experimental values are close to 20-21 G, which would seem to be explained by an increase in R_0 from 1.52 Å to 1.58-1.60 Å. In order to remove these remarks it is necessary to take into account thermal vibrations of molecules [101]

$$\langle R\rangle_{NMR}^{-3} = R_0^{-3}(1 - 2.52\langle\phi^2\rangle), \tag{22}$$

where $\langle\phi^2\rangle$ is the mean square deviation of the θ angle and is defined as

$$\langle\phi^2\rangle = h\nu/f[1/2 + (\exp(h\nu/kT) - 1)^{-1}],$$

where h is the Planck constant; ν is the frequency of librational vibrations; f is the respective force constant; k is the Boltzmann constant; T is the temperature. In this case it is necessary to qualitatively take into account $\langle\phi^2\rangle$ values, based on the general knowledge of vibrations. On the other hand, the same vibrations result in the incorrect measurement of R_0 in the diffraction experiments, too [102]

$$\langle R\rangle_X = R_0\langle\cos\phi\rangle\rangle \approx R_0(1 - \langle\phi^2\rangle/2). \tag{23}$$

Taking into account both dependences (22) and (23) and using the experimental values of $\langle R\rangle_{\mathrm{NMR}}$ and $\langle R\rangle_X$ it is possible to find the amplitude of thermal vibrations $\langle\phi^2\rangle$ and the true value of R_0 [103].

Convergence of diffraction and ^{1}H NMR *data in lawsonite*

Lawsonite $CaAl_2[Si_2O_7](OH)_2H_2O$ is the mineral characterized by the space group *Cmcm* at $T = 298$ K; *Pmcn* at $T = 233$ K, and $P2_1cn$ below 155 K. The high-temperature phase with the space group *Cmcm* is characterized by a disordered state of the hydrogen-containing sublattice and is a convenient object for the application of equations (22) and (23), the determination of the amplitude of thermal vibrations $\langle\phi^2\rangle$, and the true value of R_0. Fig. 13 shows the expected $\langle\phi^2\rangle$ values for the observed diffraction and NMR data on $\langle R\rangle$ for H_2O molecules. The convergence point $R_0 = (1.44\pm0.04)$ Å, and $\langle f_0^2\rangle = (0.38\pm0.10)$ rad^2 [56].

Comparison of neutron diffraction and ^{1}H NMR *data in edingtonite*

Edingtonite $Ba_4Al_2Si_3O_{19}\cdot4H_2O$ is a zeolite that at room temperature is characterized by the orthorhombic symmetry with the space group $P2_12_12$. The calorimetry [58], permittivity [59], and NMR [40] studies detected a phase transition near 200 K. The comparison of neutron diffraction and ^{1}H and ^{2}H NMR data shows that the low-temperature phase is incomparable and is associated with a shift of one position of the hydrogen atom of water molecules [54]. The use of formulas (22) and (23) revealed the anomalous mean square amplitude of angular vibrations for this molecule $\langle f_0^2\rangle = 0.1$ rad^2, whereas for another the similar amplitude reaches $\langle f_0^2\rangle = 0.04$ rad^2 [54].

Dependence of the amplitude of angular vibrations on the concentration of water molecules

An interesting feature of the behavior of water molecules in the laumontite↔leonhardite system (see page 226) turned out to be that the mean square amplitude of angular vibrations $\langle\theta^2\rangle$ depends on the concentration n of water molecules (Fig. 14). At a water concentration $n \sim 14.4$, which corresponds to a mixture of two phases (laumontite 40% and leonhardite 60%), the parameter $\langle\theta^2\rangle$ reaches the maximum and indicates the maximum degree of fluctuations of water molecules in vicinity of the laumontite↔leonhardite phase transition.

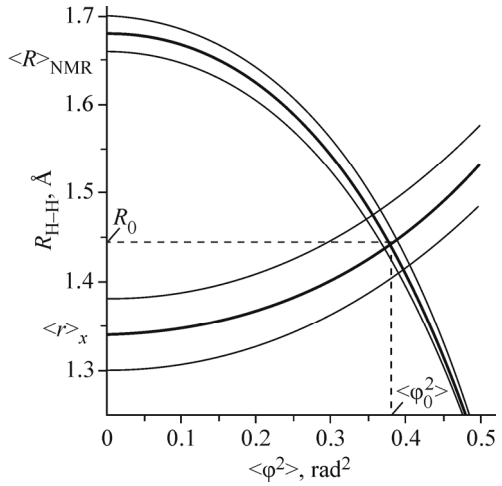

Fig. 13. Convergence of the diffraction and NMR data in lawsonite, taking into account H_2O librations in accordance with formulas (22) and (23).

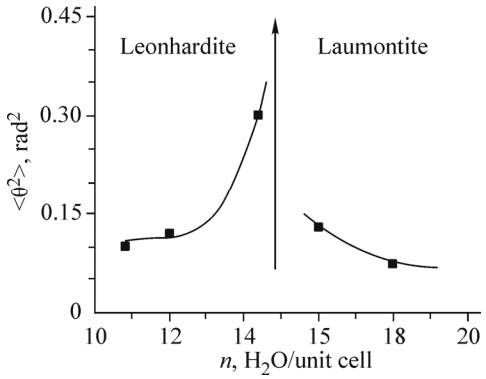

Fig. 14. Dependence of the mean square amplitude of angular vibrations $\langle\theta^2\rangle$ on the concentration of water molecules in the laumontite–leonhardite system. An arrow shows the tendency $\langle\theta^2\rangle \approx \pi$.

TABLE 1. Characteristics of ^{1}H NMR Spectra in the Heulandite Single Crystal $Na_{1.46}K_{0.23}Ca_{3.44}[Al_{8.55}Si_{23.44}O_{72}]\cdot 23.99H_2O$ (deposit on the Nidym River, Russia)

Sample	$2<h^{loc}>$, G	η	$\langle\theta^2\rangle$, rad^2
Kept for 6 h in the air at 373 K	8.3	0.093	0.12
Novosibirsk, rel. humidity 14%, 298 K	7.9	0.070	0.15
Kept in the water atmosphere with a rel. humidity 100%, 298 K	7.2	0.069	0.22

$\langle\theta^2\rangle$ is the disorder parameter of H_2O molecules; $\eta = (2\langle h_{xx}^{loc}\rangle - 2\langle h_{zz}^{loc}\rangle/2\langle h_{yy}^{loc}\rangle)$ is the asymmetry parameter; $2\langle h_{ii}^{loc}\rangle$ are doublet splittings at the orientation of the external magnetic field along *x*, *y*, *z* directions.

The dependence of $\langle\theta^2\rangle$ on the concentration *n* and pressure of water vapor in the surrounfing medium is a coomon property of the behavior of water molecules in zeolites. For narrow-pore zeolite natrolite $Na_2Al_2Si_3O_{10}\cdot 2H_2O$ it was detected with an increase in the pressure [50, 55, 60]. The same effect is observed in heulandite $Ca_4Al_8Si_{28}O_{72}\cdot 24H_2O$ (Table 1) [103], in clinoptilolite $Na_3CaAl_6Si_3O_{72}\cdot 21H_2O$ [64], and in other zeolites but is not observed in crystal hydrates of the gypsum type [101].

This type of the behavior of the vibrational amplitude of water molecules appears to be due to the entrance of water into zeolite channels or hydration. An increase in the intensity of NMR signals and the weighing of hydrated samples also support this. For natrolite at a pressure above 8 kbar the total intensity of the signal increases by 50 % [55, 60], and hence, the hydration effect cannot be considered to be small and it is possible to speak even about anomalous hydration. It is typical that in the absence of water in the surrounding medium (when fluorinated oil whose molecules cannot penetrate into zeolite channels is used) no changes occur in the NMR spectra in the same pressure range [55, 60].

The observed effect of an increase in the amplitude of molecular vibrations of zeolite water molecules with an increase in hydration can be explained by the following. In the structure of zeolites water molecules are located in potential wells [91]. If all energetically favorable positions are occupied, then the incorporation of additional molecules can occur only due to the occupation of interstices and the partial displacement of the nearest water molecules from the energetically favorable positions at the bottom of potential wells to less energetically favorable. Therefore the observed smooth decrease in the doublet splitting in the NMR spectrum and the related increase in the vibrational amplitude of water molecules reflects the degree of disorder: a shift of molecules and an increase in their potential energy due to the work of external forces.

An increase in the amplitude of molecular librations can also be observed during dehydration. For instance, in a crystal of potassium hexafluorostannate monohydrate $K_2SnF_6\cdot H_2O$ at the phase transition from the low-temperature α-phase to the β-phase near ~200 K there is a jump in $\langle\theta^2\rangle$ values increasing with an increase in the temperature from 0.13 rad^2 to 0.17 rad^2, which significantly exceeds this parameter $\langle\theta^2\rangle$ = 0.01-0.03 rad^2 common for the majority of [101] crystal hydrates (Fig. 15). With an increase in the temperature the splitting of doublets and their intensities decrease, which gives evidence of sample dehydration and an increase in the amplitude of librations of the remaining water molecules. In the range ~400-410 K, ^{1}H NMR spectra are the superposition of two doublets, the mean square amplitude of librations $\langle\theta^2\rangle \approx 0.21$ corresponding to the narrower one. The temperature dependence of the intensity of the mentioned doublets makes it possible to assume the narrow doublet to belong to the practically anhydrous γ-phase ($K_2SnF_6\cdot$[*], where the sign [*] means a water vacancy wherein a weak signal from water molecules was still observed). The results of the analysis of the angular dependence of the ^{1}H NMR spectra of $K_2SnF_6\cdot H_2O$ and practically anhydrous $K_2SnF_6\cdot$[*] indicate that under ambient conditions water molecules are orientationally disordered in this crystal and not hydrogen bonded with anions, and this disorder increases as the system is more and more dehydrated [32]. An anomalous increase in the vibrational amplitude of water molecules is explained by a degree of disorder due to a change in intermolecular interactions.

Electron correlations or vibronic interactions

Whether the electron motion affect the dynamics of atoms (vibronic interactions), be an additional mechanism for averaging the local magnetic fields or not, and how it can be detected and estimated (Prof. S. P. Gabuda)?

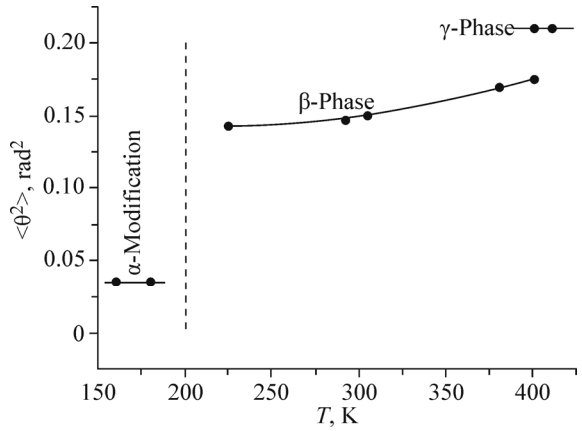

Fig. 15. Temperature dependence of the orientational disorder parameter of **p–p** vectors ($\langle\theta^2\rangle$) in the $K_2SnF_6 \cdot H_2O$ structure.

Mobility of hydrogen atoms in vanadate crystal hydrates

Vanadates are often called the salts of non-isolated vanadium acids [104]. At elevated temperatures in vanadate crystal hydrates of *ns* elements the pronounced proton dynamics is observed, which can be related to proton exchange reactions in a solid, which are accompanied by the formation of acidic and basic groups [88].

In the investigation of the electronic structure of vanadate hydrates of *s* elements and model HMO_3 and H_3MO_4 (M = V, P, As) molecules [105] it is found that at the qualitative level the temperatures (T) of phase transitions and dehydration processes in hydrovanadates and hydrophosphates are inversely proportional to excitation energies (ΔE) to the first unoccupied level

HPO_3: ΔE = 5.05 eV and T = 123 K;

$HAsO_3$: ΔE = 3.74 eV and T = 97 K;

HVO_3: ΔE = 2.34 eV and T = 383 K.

In accordance with the theory of vibronic interactions this result can give evidence of a significant role of excited electronic states in the mechanism of the appearance of proton dynamics and phase transitions in the systems under study [106]. The mixing of the ground and excited states in such systems can cause psedo-degeneration in the transition state region and also spontaneous symmetry lowering and phase transitions due to the Jahn–Teller pseudoeffect.

Table 2 lists the energy contributions to the electronic part of the formation of molecules (ZPE is the zero potential energy, Δ(RHF) is the energy obtained from the Hartree–Fock equation, Δ(LMP2) is the correlation interaction energy calculated by the local second order Möller–Plesset method. The results of the calculations demonstrate the occurrence of a dramatic increase in the contribution of correlation interactions on passing from phosphorus and arsenic *meta*- and *ortho*-acids to hypothetical vanadium *meta*- and *ortho*-acids. The found dramatic increase in the electron correlatios contributions indicate substantial changes in the character of electron delocalization in HVO_3 and H_3VO_4 molecules in comparison with

TABLE 2. Formation Energy (eV) of HMO_3 and H_3MO_4 Molecules

Molecule	Δ(LMP2)	Δ(RHF)	δ = Δ(LMP2 – – RHF)	ZPE	Molecule	Δ(LMP2)	Δ(RHF)	δ = Δ(LMP2 – – RHF)	ZPE
HPO_3	–26.1	–20.9	–5.2	0.68	H_3PO_4	–39.4	–32.8	–6.6	1.34
HVO_3	–29.9	–15.9	–14.1	0.56	H_3VO_4	–42.4	–28.0	–14.5	1.19
$HAsO_3$	–22.9	–16.3	–6.6	0.54	H_3AsO_4	–35.9	–28.3	–7.6	1.24

HPO_3 and H_3PO_4 molecules. Obviously, the obtained result is associated with the mixing of the ground and excited states or the formation of molecular orbitals which involve unoccupied 3*p* and 4*p* orbitals of P and As ions and 3*d* orbitals of V^{5+} ions. Since in the latter case the energy gaps between the unoccupied 3*d* orbitals and the energy nearest occupied states turn out to be the least, for vanadates the mixing of the ground and excited states proves to be most considerable, which provides almost half of the total binding energy in hydrovanadates.

According to Table 2 data, the binding energies calculated by the restricted Hartree–Fock method of model molecules Δ(RHF) can be considered as the values corresponding to the transition states of the systems under study in which the electron correlation contribution is as if excluded. A transition to more stable states in which the effects of mixing of states and electron correlations are taken into account within the Möller–Plesset method corresponds to a change in some generalized coordinate. For the considered systems the changes in the angular value Δφ(M–O–H), accompanying the transition to states with maximum binding energies, are most considerable. It is obtained that the absolute Δφ values of 2.43° for arsenates, 2.53° for phosphates, and 4.00° for vanadates correlate with the temperatures of the onset of proton diffusion. This is some evidence of the relationship between the mobility of hydrogen atoms in oxide systems and the contribution of electron correlation interactions.

Formulation of the theoretical model of the vibronic interaction in hydrogen-containing systems

Thus, the question arises whether electron correlations can affect the mobility of hydrogen atoms or not? Therefore, in order to answer this question the problem of particle motion in a rapidly oscillating field is considered (Fig. 16). In the approach proposed a slow system is presented by hydrogen atoms and a rapid one by the electronic motion of the hydrogen-containing matrix that can contain oxygen, carbon, nitrogen, and other neighboring atoms bound to the hydrogen atom.

The interactions of the relatively slow vibrational motion of nuclei (hydrogen) with a rapid electron motion (vibronic interaction) are taken into account with the use of the effective energy potential for this system [107]

$$U_{\text{eff}} = A[-\cos(\varphi - \varphi_0) + \pi^2((d\cdot\nu_{\text{ocs}})/(D\cdot\nu_{\text{libr}}))^2\sin^2(\varphi - \varphi_0)], \quad (24)$$

where A is the energy constant; $\nu_{\text{libr}} = 4.2\cdot10^{13}$ Hz (~1500 cm^{-1}) is the frequency of librational vibrations of OH groups, which is found from the spectroscopic data; ν_{ocs} is the frequency of electron oscillations, which is determined by the value of correlation interactions (δ) per O–H bond ($\nu_{\text{ocs}} = \delta/h$, h is the Planck constant); d is the vibrational amplitude of the electron density on oxygen atoms; D is the O–H distance; φ is the deviation angle from the equilibrium point; φ_0 is the initial (equilibrium) value of the M–O–H angle. The shortening of the O–H bond length due to the stretching vibrations of OH groups (~$1.1\cdot10^{14}$ Hz) is neglected. The first summand in equation (24) is the usual vibrational potential in the equilibrium position regardless of the effect of the oscillating field. The second summand in the addition to the potential energy

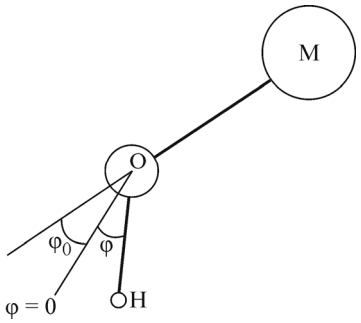

Fig. 16. Model of vibrations of the OH group: φ is the deviation angle from the equilibrium position (φ = 0); $\varphi_0 = 180° - \angle\text{MOH}$. M is the atom to which the oxygen atom is coordinated (general case).

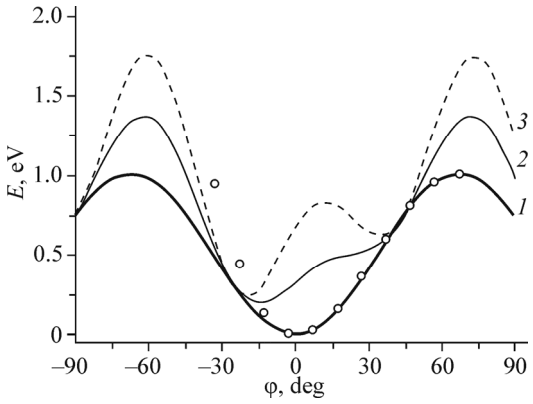

Fig. 17. Effective potential energies calculated from expression (24): calculation was performed taking into account only the first term of expression (24) (*1*); calculation was performed taking into account all contributions for the $H_2C_4O_4$ molecule (ν_{ocs} = = $7.8 \cdot 10^{14}$ Hz, $\nu_{libr} = 1.2 \cdot 10^{13}$ Hz, $d = 0.015$ Å, D = = 0.98 Å) (*2*); calculation was performed taking into account all contributions for the $D_2C_4O_4$ molecule ($\nu_{ocs} = 7.8 \cdot 10^{14}$ Hz; $\nu_{libr} = 0.85 \cdot 10^{13}$ Hz, $d = 0.015$ Å, $D = 1.20$ Å) (*3*); calculations performed by means of density functional theory, for the potential energy at a deviation of the φ angle from the equilibrium value φ = 0 in the $H_2C_4O_4$ molecule (○).

determined by rapid electron oscillations, which is due to the correlation excitations of electrons. Thus, the solution of the mechanical problem [107] is proposed to be applied to dynamic processes and structural rearrangements of molecular systems.

Proton conductor $H_2C_4O_4$

The crystal structure of high-temperature square acid (1,2-dihydroxy-3-cyclobutene-3,4-dion, $H_2C_4O_4$) is tetragonal above $T_c \approx 373$ K with the space group $I4/m$. The symmetry of the $H_2C_4O_4$ molecule is determined by the point group $4/m$; two hydrogen atoms are disordered over four equivalent positions in the plane of $(H_{1/2})_4C_4O_4$ molecules. High-resolution ^{13}C and ^{17}O NMR studies show that $H_2C_4O_4$ molecules do not have the $4/m$ symmetry in the paraelectric phase (above T_c). The symmetry lowering can be caused by weak variations in the occupation of the positions of hydrogen atoms or distortions in the C_4O_4 group. A theoretical explanation of the reasons for these distortions has not been proposed so far.

In [108] the mobility of hydrogen atoms in $H_2C_4O_4$ crystals (square acid) was studied theoretically and by the use of equation (24) the explanation of the anomalous isotopic effect was obtained for the first time: for $H_2C_4O_4$ the temperature of the transition to the hydrogen-disordered state was ≈370 K, and for $D_2C_4O_4$ it is ≈510 K. It has previously been shown [109] that for this system the model of tunneling of hydrogen atoms does not explain the experimental data. A new model is based on the theory of electron correlation interactions and the representations of the occurrence of a special vibronic interaction between the fast electron motion and a relatively slow motion of hydrogen atoms (Fig. 17).

It is seen that for the transition to the activated state in $D_2C_4O_4$ it is required to overcome a barrier of ≈0.5 eV, whereas in $H_2C_4O_4$ it is required to overcome a barrier of ≈0.25 eV (Fig. 17). From here a considerable increase in the phase transition temperature can be expected in the deuterated sample.

Thus, it is possible to suppose that electron correlations can affect the local magnetic fields of resonating nuclei and make them decrease. However, it should be noted that the model proposed needs additional elaboration and development. Some more examples of the application of the approach proposed can be found in [110, 111].

CONCLUSIONS

The presented results of persistent and numerous studies of Prof. S. P. Gabuda demonstrates the exclusive fruitfulness of the NMR method when the vacancy model of averaging local magnetic fields $\langle h^{loc} \rangle$ is applied for the investigation of intracrystal molecular mobility. The proposed model is valid because the spectral shapes of ^{1}H NMR lines calculated from it and their angular dependences with respect to the external magnetic field correspond to the observed spectral lines in both crystal hydrates and zeolites as well as clays and biological tissues. The structural aspects of the model enable the analysis of the observed ^{1}H NMR spectra not only in accordance with the crystal symmetry but also the analysis of the phenomena such as phase transitions in molecular guest subsystems of crystals. It also makes it possible to reveal the degree of disorder in the subsystem of guest molecules and the relationship between the disorder and the processes of intermolecular interactions and molecular sorption. These items belong to the fundamental problems of solid physics and chemistry and deal with their practically important characteristics (ferroelectricity, plasticity, thermodynamic properties, etc.).

The further development of this model can be associated with the clarification of the role of electron correlations in the location and mobility of hydrogen atoms and molecules. To this end, the theoretical model has been formulated within which a shematic relationship between the electronic structure of hydrogen-containing systems and the mobility of hydrogen atoms in them was proposed. The model is based on the theory of electron correlation interactions and the representations of the occurrence of a vibronic interaction between the fast electron motion and a relatively slow motion of nuclei, in particular, hydrogen atoms. The elucidation of this problem will make it possible to more exactly determine the mechanisms resulting in the intracrystal mobility of atoms and molecules.

Note that this review does not mention all NMR studies of the mobility of atoms and molecules, which Prof. S. P. Gabuda performed. In particular, it does not present the studies on the mobility and location of fluorine atoms in transition metal and lanthanide hexafluorides and also other atoms in various classes of compounds [112-115].

The authors are grateful to O. V. Falaleev for valuable remarks during the work on this review.

REFERENCES

1. A. Abraham, *Nuclear Magnetism*, Oxford University Press, Oxford (1961).
2. C. P. Slichter, *Principles of Magnetic Resonance*, Harper, New York (1964).
3. N. Bloembergen, E. M. Pursell, and R. V. Pound, *Phys. Rev*., **73,** 679 (1948).
4. G. E. Pake, *J. Chem. Phys*., **16,** 327 (1948).
5. S. Yano, *J. Phys. Soc. Jpn*., **14,** 942 (1959).
6. X. Pare, *C. R. Acad. Sci*., **254,** 1617 (1962).
7. T. Tsang and D. E. O′Reilly, *J. Chem. Phys*., **43,** 4234 (1965).
8. S. P. Gabuda and A. F. Rzhavin, *Niclear Magnetic Resonance in Crystal Hydrates and Hydrated Proteins* [in Russian], Nauka, Novosibirsk (1978).
9. P. Ducros, *Bull. Soc. Fr. Mineral. Cristallogr*., **83,** 85 (1960).
10. S. P. Gabuda and A. G. Lundin, *JETP*, **28**, No. 3, 555 (1969).
11. S. P. Gabuda, *NMR Study of Weak Interactions in Crystals* [in Russian], Doctoral (Phys.-Math.) Dissertation, Novosibirsk (1969).
12. H. S. Gutowsky and G. E. Pake, *J. Chem. Phys*., **18,** 162 (1950).
13. S. P. Gabuda, R. N. Pletnev, and M. A. Fedotov, *Nuclear Magnetic Resonance in Inorganic Chemstry* [in Russian], Nauka, Moscow (1988).
14. S. P. Gabuda and A. G. Lundin, *Internal Mobility in Solids* [in Russian], Nauka, Novosibirsk (1986).
15. N. A. Sergeev, O. V. Falaleev, and S. P. Gabuda, *Fiz. Tv. Tela*, **11,** 2248 (1969).

16. S. P. Gabuda, L. V. Ivleva, and A. G. Lundin, *J. Struct. Chem*, **11**, No. 4, 600 (1970).
17. N. A. Sergeev, *J. Struct. Chem*., **23**, No. 4, 554 (1983).
18. A. G. Lundin and S. P. Gabuda, *Dokl. Akad. Nauk SSSR*, **178,** 641 (1968).
19. K. S. Aleksandrov, S. P. Gabuda, G. M. Mikhailov, and A. G. Lundin, *Izv. Akad. Nauk, Ser. Fiz*., **24**, No. 10, 1195 (1960).
20. K. S. Aleksandrov, S. P. Gabuda, and A. G. Lundin, *Izv. Akad. Nauk, Ser. Fiz*., **29**, No. 6, 907 (1965).
21. S. P. Gabuda, G. M. Mikhailov, A. G. Lundin, and K. S. Aleksandrov, *Dokl. Akad. Nauk SSSR*, **141**, No. 6, 1406 (1961).
22. A. G. Lundin, G. M. Mikhailov, and S. P. Habuda, *JETP*, **13**, No. 5, 903 (1961).
23. G. M. Mikhailov, A. G. Lundin, and S. P. Gabuda, *JETP*, **14**, No. 5, 977 (1962).
24. S. P. Gabuda, G. M. Mikhailov, and A. G. Lundin, *Dokl. Akad. Nauk SSSR*, **136**, No. 4, 864 (1961).
25. S. P. Gabuda, Yu. V. Gagarinskii, S. A. Durasova, and A. G. Lundin, *J. Struct. Chem*., **5**, No. 2, 273 (1964).
26. S. P. Gabuda, Yu. V. Gagarinskii, and G. M. Mikhailov, *J. Struct. Chem*., **5**, No. 3, 357 (1964).
27. A. G. Lundin, S. P. Gabuda, and E. P. Zeer, *JETP Lett.*, **9**, No. 7, 259 (1969).
28. A. G. Lundin, E. P. Zeer, and S. P. Gabuda, *Izv. Akad. Nauk, Ser. Fiz*., **33**, No. 2, 261 (1969).
29. S. P. Habuda, A. G. Lundin, and E. P. Zeer, *Ferroelectrics*, **1,** 71 (1970).
30. S. P. Habuda and J. V. Gagarinskij, *Acta Crystallogr. B*, **27,** 1677 (1971).
31. N. A. Sergeev, E. M. Kiperman, A. M. Vakhrameev, and M. L. Afanas′ev, *J. Struct. Chem*., **22**, No. 2, 212 (1981).
32. V. Ya. Kavun, S. P. Gabuda, A. V. Gerasimenko, G. L. Trofimov, and I. A. Tkachenko, *J. Struct. Chem*., **43**, No. 2, 355 (2002).
33. S. P. Gabuda, *Dokl. Akad. Nauk SSSR*, **146**, No. 4, 840 (1962).
34. S. P. Gabuda and G. M. Mikhailov, *J. Struct. Chem*., **4**, No. 3, 404 (1964).
35. S. P. Gabuda, G. M. Mikhailov, and N. S. Aleksandrov, *Dokl. Akad. Nauk SSSR*, **153**, No. 6, 1360 (1963).
36. S. P. Gabuda, G. M. Mikhailov, and A. G. Lundin, *Geokhimiya*, **4,** 463 (1963).
37. S. P. Gabuda, G. M. Mikhailov, and A. G. Lundin, *Kristallografiya*, **8**, No. 3, 388 (1963).
38. S. P. Gabuda, I. A. Belitskii, and G. V. Bukin, *Dokl. Akad. Nauk SSSR*, **159**, No. 5, 1038 (1964).
39. S. P. Gabuda, G. M. Mikhailov, and K. S. Aleksandrov, *Dokl. Akad. Nauk SSSR*, **153**, No. 6, 1360 (1964).
40. I. A. Belitskii, S. P. Gabuda, and A. G. Lundin, *Dokl. Akad. Nauk SSSR*, **172**, No. 6, 1318 (1967).
41. V. F. Ivleva, N. I. Zavarzina, and S. P. Gabuda, *Kristallografiya*, **13**, No. 4, 815 (1968).
42. N. I. Zavarzina and S. P. Gabuda, *Izv. Akad. Nauk, Ser. Fiz*., **33**, No. 2, 258 (1969).
43. L. V. Ivleva, S. P. Gabuda, and A. G. Lundin, *J. Struct. Chem*., **10**, No. 5, 690 (1969).
44. N. I. Zavarzina, S. P. Gabuda, V. V. Bakakin, and G. M. Rylov, *J. Struct. Chem*., **10**, No. 5, 696 (1969).
45. L. V. Ivleva and S. P. Gabuda, *Kristallografiya*, **16**, No. 4, 825 (1971).
46. I. V. Grinchenko and S. P. Gabuda, *J. Struct. Chem*., **12**, No. 1, 28 (1971).
47. V. Yu. Galitskii, V. N. Shcherbakov, and S. P. Gabuda, *Kristallografiya*, **17**, No. 4, 788 (1972).
48. L. V. Kashkina and S. P. Gabuda, *J. Struct. Chem*., **13**, No. 6, 949 (1972).
49. L. V. Ivleva, A. M. Vakhrameev, and S. P. Gabuda, *J. Struct. Chem*., **14**, No. 1, 38 (1973).
50. I. A. Belitskii, V. N. Shcherbakov, and S. P. Gabuda, *Dokl. Akad. Nauk SSSR*, **208**, No. 5, 671 (1973).
51. I. A. Belitskii, V. N. Shcherbakov, S. P. Gabuda, and L. D. Filizova, *J. Struct. Chem*., **14**, No. 6, 964 (1973).
52. S. P. Gabuda and A. A. Matsutsin, *J. Struct. Chem*., **17**, No. 5, 710 (1976).
53. A. V. Sapiga, N. A. Sergeev, V. N. Shcherbakov, S. P. Gabuda, and I. A. Belitskii, *J. Struct. Chem*., **27**, No. 4, 666 (1986).
54. I. A. Belitsky, S. P. Gabuda, W. Joswig, and H. Fuess, *Neues Jahrb. Mineral., Abh*., **12,** 541 (1986).
55. I. A. Belitsky, B. F. Fursenko, S. P. Gabuda, O. V. Kholdeev, and Yu. V. Seryotkin, *Phys. Chem. Min*., **18,** 497 (1992).
56. S. G. Kozlova and S. P. Gabuda, *J. Struct. Chem*., **54**, Suppl. 1, 146 (2013).

57. S. P. Gabuda, S. G. Kozlova, A. S. Kolesnikov, and A. K. Petrov, *J. Struct. Chem*., **54**, Suppl. 1, 119 (2013).
58. E. B. Amitin, I. A. Belitskii, S. P. Gabuda, Yu. A. Kovalevskaya, O. A. Nabutovskaya, and T. M. Polyanskaya, *J. Struct. Chem*., **22**, No. 3, 441 (1981).
59. S. P. Gabuda, V. Yu. Galitsky, S. G. Kozlova, Yu. G. Kriger, and N. K. Moroz, *Ferroelectrics*, **64,** 65 (1985).
60. I. A. Belitskii, S. P. Gabuda, and N. K. Moroz, *Dokl. Akad. Nauk SSSR*, **292**, No. 5, 1232 (1987).
61. A. M. Panich, I. A. Belitskii, N. K. Moroz, S. P. Gabuda, V. A. Drebushchak, and Yu. V. Seretkin, *J. Struct. Chem*., **31**, No. 1, 56 (1990).
62. D. Kirov, L. Filizova, S. P. Gabuda, S. G. Kozlova, and N. K. Moroz, *J. Struct. Chem*., **34**, No. 3, 390 (1993).
63. S. P. Gabuda and S. G. Kozlova, *J. Inclusion Phenom*., **22**, No. 1, 1 (1995).
64. S. P. Gabuda, S. G. Kozlova, D. G. Kirov, L. D. Filizova, and V. V. Lisin, *J. Struct. Chem*., **37**, No. 5, 759 (1996).
65. S. P. Gabuda, S. G. Kozlova, and N. K. Moroz, *Nat. Zeolites*, G. Kirov, L. Filizova, and O. Petrov (eds.), Sofia′95 (1997).
66. S. P. Gabuda and S. G. Kozlova, *J. Struct. Chem*., **38**, No. 4, 562 (1997).
67. S. P. Gabuda, S. G. Kozlova, and A. G. Lundin, *Zh. Fiz. Khim*., **79**, No. 3, 1 (2005).
68. S. P. Gabuda, A. S. Kolesnikov, S. G. Kozlova, A. G. Lundin, and N. K. Moroz, *Appl. Magn. Reson*., **41,** 439 (2011).
69. S. P. Gabuda, A. S. Kolesnikov, S. G. Kozlova, and N. K. Moroz, *Appl. Magn. Reson*., **41,** 431 (2011).
70. A. A. Khanagov and S. P. Gabuda, *Biofizika*, **15**, No. 5, 796 (1970).
71. S. P. Gabuda and N. V. Ratnikova, *Biofizika*, **18**, No. 6, 981 (1973).
72. A. F. Rzhavin, S. P. Gabuda, and V. N. Shcherbakov, *Biofizika*, **21**, No. 1, 21 (1976).
73. S. P. Gabuda and A. F. Rzhavin, *Mol. Biol*., **10,** 998 (1976).
74. S. P. Gabuda, Yu. P. Meshalkin, B. P. Tolochko, and G. N. Kulipanov, *Biofizika*, **29**, No. 2, 316 (1984).
75. S. P. Gabuda, A. A. Gaidash, V. A. Drebushchak, and S. G. Kozlova, *JETP Lett*., **82**, No. 9, 613 (2005).
76. S. P. Gabuda, A. A. Gaydash, V. A. Drebushchak, and S. G. Kozlova, *J. Struct. Chem*., **46**, No. 6, 1131 (2005).
77. S. P. Gabuda, A. A. Gaidash, and E. A. Vyazovaya, *Biofizika*, **50**, No. 2, 231 (2005).
78. S. P. Gabuda, A. A. Gaidash, S. G. Kozlova, and N. L. Allan, *J. Struct. Chem*., **47**, No. 2, 258 (2006).
79. M. M. Selim, S. P. Gabuda, A. M. Panich, Z. V. Gryaznova, and N. K. Moroz, *Dokl. Akad. Nauk SSSR*, **224,** 1119 (1975).
80. I. V. Grinchenko and S. P. Gabuda, *J. Struct. Chem*., **11**, No. 3, 411 (1970).
81. I. V. Grinchenko and S. P. Gabuda, *J. Struct. Chem*., **10**, No. 4, 633 (1969).
82. N. K. Moroz, A. M. Panich, and S. P. Gabuda, *J. Struct. Chem*., **19**, No. 2, 252 (1978).
83. N. K. Moroz, A. M. Panich, and S. P. Gabuda, *J. Magn. Reson*., **53,** 1 (1983).
84. A. M. Panich, A. M. Danilenko, and S. P. Gabuda, *Dokl. Akad. Nauk SSSR*, **281,** 389 (1985).
85. A. I. Rubailo, S. P. Gabuda, and V. E. Volkov, *J. Struct. Chem*., **10**, No. 4, 635 (1969).
86. A. V. Sabylinskii, S. P. Gabuda, S. G. Kozlova, D. N. Dybtsev, and V. P. Fedin, *J. Struct. Chem*., **50**, No. 3, 421 (2009).
87. S. P. Gabuda, S. G. Kozlova, D. N. Dybtsev, and V. P. Fedin, *J. Struct. Chem*., **50**, No. 5, 887 (2009).
88. S. P. Gabuda and R. N. Pletnev, *Application of NMR in Solid State Chemistry* [in Russian], Ekaterinburg (1996).
89. S. P. Gabuda, *Bound Water: Facts and Hypotheses* [in Russian], Nauka, Novosibirsk (1982).
90. W. R. Busing and H. A. Levy, *Acta Crystallogr*., **17,** 142 (1964).
91. L. Bragg and G. F. Claringbull, *Crystal Structure of Minerals*, Bell, London (1965).
92. E`. E`. Suyunova, V. V. Mank, Yu. I. Tarasevich, and A. G. Brekhunets, *Ukr. Khim. Zh*., **15,** 36 (1974).
93. V. V. Mank, S. P. Suleimanov, F. D. Ovcharenko, and N. G. Vasiliev, *Dokl. Akad. Nauk SSSR*, **224**, No. 5, 1111 (1975).
94. J. Graham, G. F. Walker, and G. W. West, *J. Chem. Phys*., **40,** 540 (1964).
95. M. E. Nimni (ed.), *Collagen I-4*, CRS Press, Boca Raton, FL (1988).

96. T. J. Wess, A. P. Hammersley, L. Wess, and A. Miller, *J. Mol. Biol*., **248,** 485 (1995).
97. D. J. S. Holmes, T. J. Wess, D. J. Prockop, and P. Fratzl, *Biophys. J*., **68,** 1661 (1995).
98. R. B. D. Frazer and B. L. Trus, *Biosci. Rep*., **6,** 221 (1986).
99. C. Migchelsen and H. J. C. Berendsen, *J. Chem. Phys*., **59,** 296 (1973).
100. G. M. Zaslavskii and R. Z. Sagdeev, *Introduction into Nonlinear Physics: from a Pendilum to Turbulance and Chaos* [in Russian], Nauka, Moscow (1982).
101. B. Pedersen, *J. Chem. Phys*., **41,** 122 (1964).
102. S. W. Peterson and H. A. Levy, *Acta Crystallogr*., **10,** 70 (1957).
103. S. P. Gabuda, S. G. Kozlova, N. K. Moroz, L. Filizova, and D. Kirov, in: *Natural Zeolite'93: Occurrence, Properties, Use*, D. W. Ming and F. A. Mumpton (eds.), International Committee on Natural Zeolites, Brockport, New York, USA (1995).
104. A. F. Wells, *Structural Inorganic Chemistry*, 5th ed., Clarendon, Oxford (1986).
105. S. P. Gabuda, S. G. Kozlova, and R. N. Pletnev, *Dokl. Akad. Nauk (Khim.)*, **413**, No. 6, 1 (2007).
106. I. B. Bersuker, *The Jahn-Teller Effect and Vibronic Interactions in Modern Chemistry*, Plenum, NY (1984).
107. L. D. Landau and E. M. Lifshitz, *Theoretical Physics, Mechanic*, vol. 1, Pergamon Press, Oxford (1981), chap. 5.
108. S. P. Gabuda, S. G. Kozlova, and N. Dalal, *Solid State Comm*., **130,** 729 (2004).
109. E. J. Samuelsen, U. Bucchenau, M. Dieter, K. Ehrhardt, E. Fjaer, and H. Grimm, *Phys. Scr*., **25,** 685 (1982).
110. S. P. Gabuda and S. G. Kozlova, *Lone Pairs and Chemical Bonding in Molecular and Ionic Crystals* [in Russian], V. M. Buznik (ed.), Izd. SO RAN, Novosibirsk (2009).
111. E. I. Yuryeva, S. P. Gabuda, and R. N. Pletnev, *Quantum Chemistry and Nuclear Resonance Spectroscopy Data of Natural and Synthetic Nanotechnological Materials with nd-Metal Atoms Participations*, E. O. Hoffman (ed.), Nova Science Publishers, NY (2007).
112. S. P. Gabuda and S. V. Zemskov, *Nuclear Magnetic Resonance in Complex Compounds* [in Russian], B. I. Peshchevitskii (ed.), Nauka, Novosibirsk (1976).
113. S. P. Gabuda, Yu. V. Gagarinskii, and S. A. Polishchuk, *NMR in Inorganic Fluorides: Structure and Chemical Bonding* [in Russian], Atomizdat, Moscow (1978).
114. S. P. Gabuda and R. N. Pletnev, *Application of NMR in Solid State Chemistry* [in Russian], Ekaterinburg (1996).
115. S. P. Gabuda and S. G. Kozlova, *NMR, Magnetic Behavior and Structural Effects of Spin-Orbit Interactions in PtF_6 and in Related Octahedral Molecules and Fluorocomplexes*, in: *Handbook of Inorganic Chemistry Research*. *Chemistry Research and Applications*, D. A. Morrison (ed.), Nova Science Publishers, NY (2010).